THE BLENDING OF HYDROXYPROPYL LIGNIN WITH POLY(METHYL METHACRYLATE) AND POLY(VINYL ALCOHOL)

by

Scott Leonard Ciemniecki

Thesis submitted to the Faculty of the
Virginia Polytechnic Institute and State University
in partial fulfillment of the requirements for the degree of

Master of Science
in
Forest Products

Approved:

W. G. Glasser, Chairman

G. L. Wilkes

T. C. Ward

August, 1986

Blacksburg, Virginia

The Blending of Hydroxypropyl Lignin with Poly(methyl methacrylate) and Poly(vinyl alcohol)

by

Scott Leonard Ciemniecki

(ABSTRACT)

Polymer blends consisting of hydroxypropyl lignin (HPL) and commercially available poly(methyl methacrylate) (PMMA) and poly(vinyl alcohol) (PVA) were evaluated in terms of their morphology, viscoelastic properties and mechanical properties.

In the case of HPL/PMMA blends experimental variables included HPL molecular weight, HPL content and method of preparation. Methods of preparation included injection molding and solution casting with THF (a hydrogen bonding solvent) and chloroform (a non-hydrogen bonding solvent). SEM results indicated that all HPL/PMMA blends formed two phase systems. However the domain-matrix interphase varied with the method of preparation and HPL molecular weight. Most notably was that solution cast blends showed domains that were "pulled away" from the matrix whereas injection molded blends showed HPL striations that were closely associated with the matrix. Injection molded blend's T_g values were found to more closely follow predicted T_g values (Flory-Fox equation) and injection molded blends also showed consistently superior material properties.

Polymer blends of HPL and PVA were prepared by solution casting and evaluated in terms of HPL content and PVA's solubility parameter.

Blends of HPL and PVA formed homogeneous materials over a much broader range of solubility parameters than would be predicted from the theory of matching solubility parameters. It was concluded that hydrogen bonding between hydroxyl groups on both polymers was responsible for the formation of at least partially miscible systems over a wider than expected range of solubility parameters.

Acknowledgements

I would like to express my appreciation to the many people who contributed to the completion of this project. Sincere gratitude goes to my major professor, Wolfgang G. Glasser, who has given generously of his expertise, time and patience over the past two years. His encouragement and support have enabled me to grow both professionally and personally. I would also like to thank my committee members, Dr. T. C. Ward and Dr. G. Wilkes, whose helpful suggestions and feedback greatly improved this study.

I wish to thank Myrtle for her time and talents without which this thesis would not have been completed on time.

A special note of thanks goes to my colleagues, the faculty and staff in the Department of Forest Products, who I have had the pleasure of working and socializing with for a unique experience and many fond memories. I also wish to thank a special groups of friends - Carlile, Steve and T.C. for their friendship, sometimes valuable criticism, and always helpful diversions.

Words seem petty when I try to express my thanks and feelings for my brothers - Bruce and Kip, my sisters - Sharon and Laura, my mother and the rest of my family whose confidence in my abilities and support was always unwavering.

Preface

The two chapters of this thesis have been prepared as manuscripts which will be submitted for publication. As such, each chapter has its own introduction, experimental section and literature citations. This type of format unavoidably introduces a certain amount of duplication which could prove somewhat redundant for the reader of this work. Apologies are made if this appears inconvenient.

Table of Contents

LITERATURE REVIEW

A. Thermosetting Structural Polymers from Lignin

Lignin is a polymeric organic substance which comprises about 20 to 30 percent of the dry plant material (1). The biosynthesis of lignin from monomeric phenyl propane units, coniferyl alcohol, sinapyl alcohol, and para-coumaryl alcohol, can be generally described as a dehydrogenative polymerization. The build-up of lignin macromolecules within a plant is a complicated biological process which has been extensively studied and reviewed (2-7). Within the plant, lignin in conjunction with hemicelluloses, makes up an amorphous matrix in which crystalline cellulose is imbedded. Lignin functions as an anti-oxidant, as a barrier against biological decay, and as a structural support matrix. As a support matrix lignin increases the mechanical strength properties to such an extent that plants such as trees can obtain heights above 100 meters.

Lignin may be isolated as a by-product of the pulp and paper industry, and it remains an under-utilized material. Currently, most lignin serves as an inexpensive, in-mill source of energy where it has a fuel equivalent of about two cents per pound (8). Some lignins such as lignosulphonates have been utilized as drilling mud additives, as cement additives, and as binders, but the amount utilized represents only ca. 25% of total lignosulphonate production (9). As in the case of lignin as an energy source these lignosulphonate markets represent relatively low value markets, that is an annual production of 1.5 x 10^9 lbs has a value of \$180 x 10^6 (10). High value markets such as

those represented by adhesives and plastics have not been successfully entered due to three main reasons. First, the inability to fully describe the structure of lignin. Secondly, the inherent variability of lignin, and third, the resistance of lignin to many types of degradation (11). The development of novel biomass conversion technologies has helped stimulate renewed interest in utilizing lignin in high value markets. These biomass conversion technologies, which include organosolv pulping and steam explosion pulping, are dependent on the utilization of the lignin-rich residue in high value markets (12). As a result, current lignin research has concentrated on taking advantage of lignin as a polymeric material.

When attempting to engineer novel plastics it should be understood that there are at least four ways to formulate polymeric materials with unique properties: (1) develop new monomers, (2) develop new methods and techniques of polymerization, (3) combine existing monomers in such a way that the resulting materials have certain superior properties, and (4) combine existing polymers in unusual ways to achieve new and useful properties. Past research involving engineering plastics from lignin centered mainly on procedures 1, 2 and 3 where lignin was viewed as the initial polyol "monomer" in the formation of polyurethane and phenol formaldehyde networks. In the case of polyurethanes initial research at Virginia Tech prepared lignin-based polyurethane films by crosslinking with diisocyanates (13,14). In a series of studies crosslinking variables such as crosslinking agent, crosslinking density, soft segment type and soft

segment weight fraction were investigated. The greatest influence on crosslink density was seen up to a NCO:OH ratio of three, where the maximum effective crosslinking occurred. Similarly, the T_g's of the films showed a rapid increase as NCO:OH ratio increased until plateauing above a ratio of three. It was also found, that films prepared with aliphatic polyisocyanates yielded materials that ranged from brittle to tough. In a second study the effects of crosslink density were investigated. The crosslink density was regulated by altering the hydroxyl content of the hydroxypropyl lignin by a reaction with butylisocyanate. The authors concluded that the reaction between mono-isocyanates and alcohol groups provides an excellent method for reducing the hydroxy content of the lignin-derived polyols. The crosslink density of the films prepared with these polyols followed a predictable decline which coincided with the reduction of hydroxy groups. Finally, a strong linear relationship was found between the film T_g and the T_g of the polyol from which it was formulated. The overall conclusion of the study stated that opportunity exists to engineer lignin based polyurethanes with specific end-product properties.

In a related paper the introduction of a soft segment into lignin based polyurethanes was investigated by Saraf, Glasser, Wilkes and McGrath (15). In this study four polyethylene glycols (PEG) of molecular weight 400, 600, 1000 and 4000 were mixed with lignin polyol in order to incorporate different amounts of a "soft segment" into a polyurethane network. "Soft segments" derive their name from their

ability to act as a dampening mechanism, therefore toughening a material. Results indicated that the introduction of a soft segment increased the chain mobility of the network and resulted in lower mechanical relaxation and thermal transition temperatures. The energy dissipating characteristics (damping) of the films and their dependence on temperature were found to be a function of both parameters, soft segment weight fraction and soft segment molecular weight. In conclusion the results suggested that it is possible to introduce a considerable measure of toughness into thermosetting lignin-based polyurethanes by incorporating a (PEG) component of variable molecular weight and weight fraction.

In an attempt to covalently incorporate a high percentage of lignin into a phenol-formaldehyde resin Muller and Glasser first derivatized the lignin (16). The derivatization procedure involved hydroxymethylation followed by phenolation. This derivatized lignin was then used as the phenol component in a phenol-formaldehyde resin which was cooked using a conventional viscosity/time profile. Results concerning activation energies and cure rates indicated that the derivatized kraft and steam explosion lignin have no inhibitory influence on resin cure up to 50%-60% phenol substitution levels. Shear strengths of the kraft and steam explosion based PF resins compared favorably with strength values of the neat resin.

Results from the studies mentioned in this review as well as others concerning engineering plastics from lignin have revealed that lignin can be incorporated into and become an active component of

various polymer networks. These studies help support the conclusion that lignin can be analyzed, derivatized and incorporated into polymeric material systems by using classical polymer science methodology.

As stated earlier there are a number of methods for developing novel polymer materials. These methods include the development of new methods and techniques of polymerization, the combination of existing monomers in novel arrangements and the combination of existing polymers. Previous studies (involving engineering plastics from lignin) have centered around the development of new monomers, the development of new polymerization techniques and the combination of existing monomers. The present study on the other hand will explore the effect of HPL on the properties of commercially existing polymers in multiphase materials of the type of polyblends. Specifically, the following objectives can be defined:

1) To blend hydroxypropyl lignin (HPL) with commercially available poly(methyl methacrylate) (PMMA) and poly(vinyl alcohol) (PVA), and to describe the resulting materials in terms of miscibility, compatibility and material properties.

2) To determine what effect various preparation techniques have on polymer blends of HPL and PMMA. Preparation techniques are to include solution casting with tetrahydrofuran THF, (a hydrogen bonding solvent, and chloroform, a non-hydrogen bonding solvent, and injection molding. Differences are to be interpreted in terms of polymer morphology, mechanical properties, and thermomechanical properties.

3) To explore the effect of molecular weight on blend miscibility, morphology and material properties.

4) To study the effects of solubility parameter and hydrogen bonding on the miscibility of HPL/PVA polyblends. This is to involve PVA's with degrees of hydrolysis of 96%, 88% and 75%, and with solubility parameters of 12.6, 11.8 and 10.6, respectively.

B. Polymer Blends

Multicomponent polymeric systems or more simply "polyblends" received considerable interest in part because they represent an important group of thermoplastic materials and blending is a convenient way of improving material properties of simple thermoplastics. Polyblends have become an important group of thermoplastics due to the increasing difficulty and expense of developing new polymers. The blending of polymers constitutes an inexpensive way to alter the physical properties of a material without introducing new chemical structures. The altering of physical properties in polyblends occurs because for thermodynamic reasons, polymer blends do not usually form homogeneous mixtures but exhibit micro or macrophase separation. Microphase separation may exhibit domains with diameters of a few hundred angstroms whereas macrophase separation may show domains with diameters of several thousand angstroms. Therefore the blending of two polymers will usually produce a class of materials whose properties are based on the presence of two phases. On the other hand, if the polymers comprising the mixture have a strong enough affinity for one another, they will

be mutually soluble and form a homogeneous material. While such homogeneous materials are often desirable for ease of blending, some degree of heterogeneity often leads to useful properties. Whereas a completely homogeneous polyblend tends to average the properties of the two polymers comprising the polyblend, in relation to their respective weight fractions, a multiphase polyblend often provides a superior balance of useful properties. In some rare cases, synergistic effects even occur, in which one or more properties of the composite are superior to those dual components (17-18).

Thus far, for simplicity, the terms homogeneous and heterogeneous have been used to describe the phase behavior of polyblends. However before further discussing the thermodynamics and properties of polyblends, two terms, "miscibility" and "compatibility" which are more commonly used to describe phase behavior should be defined. Even though these two terms have different meanings they are commonly used interchangeably. Whereas "miscibility" is a thermodynamic term used to denote solubility at the molecular level, "compatibility" is a commercial term used to indicate the usefulness of a polyblend. Therefore immiscible blends can in certain cases exhibit good mechanical properties, and thus are said to be mechanically compatible (19).

1) Basic Thermodynamics

As mentioned earlier, polymer blends do not usually form homogeneous mixtures but exhibit micro or macrophase separation. This phase separation occurs due to the fact that when two liquids are

mixed, their miscibility depends upon a negative Gibb's free energy of mixing, ΔG, which in turn is the result of the heat of mixing, ΔH, and the product of the entropy of mixing ΔS and the absolute temperature T, as shown in equation 1.

$$\Delta G = \Delta H_{mix} - T\Delta S_{mix} \qquad \text{(Eq. 1)}$$

where ΔG = Gibb's free energy of mixing

ΔH_{mix} = Enthalpy of mixing

ΔS_{mix} = Entropy of mixing

T = Absolute temperature

Since any molecule is generally more attracted to similar molecules than to dissimilar molecules, the heat of mixing is usually endothermic and positive. When mixing small molecules of two different liquids, the increase in randomness, and thus in entropy, is high and positive allowing the $T\Delta S$ product to outweigh the endothermic heat of mixing ΔH. A negative free energy term ΔG is therefore favored and miscibility is possible. When mixing large polymer molecules, on the other hand, the thousands of atoms in each molecule must remain together, and mixing cannot be nearly as random. The gain in entropy cannot be nearly as high. Thus it is rarely possible for the $T\Delta S_{mix}$ term to exceed the endothermic heat of mixing (ΔH). This explains why very few pairs of polymers are truly miscible, in a thermodynamic sense, and do not form homogeneous, single-phase materials. In fact, in those rare cases in which complete miscibility and homogeneity do occur, they are usually due to specific interactions between the two

polymers rather than to a negative ΔG-term. These interactions may include polar attractions, hydrogen-bonding or acid-base interactions.

a) Enthalpy of Mixing

The enthalpy of mixing (ΔH_{mix}) can be formulated in terms of relative numbers of intermolecular contacts between like and unlike molecules. Non-zero ΔH_{mix} values are assumed to be caused by the net results of breaking solvent (1-1) contacts and polymer (2-2), (3-3) contacts and the creation of polymer-polymer (2-3) contacts (20, 21). In other words, the molecules to be "mixed" attract each other more than they attract their own kind. Thus it is apparent that the mixing of two components always results in a change of energy in the system. When the individual components of a mixture interact through dispersion or Van der Waals forces, the enthalpy of mixing is given by equation 2.

$$\Delta H_{mix} = (V_1 + V_2)\, B\, \phi_1\, \phi_2 \qquad \text{(Eq. 2)}$$

where $V_{1,2}$ and $\phi_{1,2}$ represent the molar volume and the volume fraction of the components 1 and 2 in the mixture, respectively. The term B is a binary interaction energy density characteristic of mixing segments of components 1 and 2. The latter is simply related to Flory's polymer interaction parameter, χ (chi) by:

$$\frac{B}{RT} = \frac{\chi_1}{V_1} = \frac{\chi_2}{V_2} = \frac{\chi_{12}}{V_u} = \chi_{12} \qquad \text{(Eq. 3)}$$

where V_u is the molar volume of an arbitrary unit of the polymer chain, R is the universal gas constant and T is the absolute

temperature. χ (chi) or the Flory-Huggins interaction parameter is defined as:

$$\chi_{1,2} = \frac{W_{1,2}\, r_1\, Z}{Kt} \qquad \text{(Eq. 4)}$$

where Z is the coordination number, W_{12} is the increase in energy when a solvent-polymer bond is formed from molecules that were originally in contact only with species of like kind, k is the Boltzman constant, and r_1 is the number of repeat units in the molecule of component 1. In short, the Flory-Huggins interaction parameter (χ) is a measure of the degree of specific interactions between mixed components.

By combining the equation for χ (equation 4) with equations 2 and 3 we get equation 5 for ΔH_{mix}.

$$\frac{\Delta H_{mix}}{V} = \frac{\chi_{1,2} RT}{V_1}\, \phi_1\, \phi_2 \qquad \text{(Eq. 5)}$$

Equation 5 establishes a relationship between the Flory-Huggins interaction parameter (χ) and ΔH_{mix}.

b) <u>The Entropy of Mixing</u>

The change in the entropy of mixing two components was predicted by Flory and Huggins based on their lattice model (22). The model considers a number of combinations that solvent and polymer molecules can be arranged in a lattice of fixed volume. The entropy change upon mixing two high molecular weight polymers is much lower than that of two low molecular weight species or solvents because the number of

possible arrangements in the case of two polymers is much more limited. However, the entropy is always positive which leads to a negative contribution to ΔG_{mix}. From the lattice analysis, the equation for the entropy of mixing, ΔS_{mix} is given by equation 6:

$$\Delta S_{mix} = -R\{N_1 \ln \phi_1 + N_2 \ln \phi_2\} \qquad \text{(Eq. 6)}$$

where $N_{1,2}$ = number of moles of solvent and polymer

$\phi_{1,2}$ = volume fraction of solvent and polymer.

The subscripts 1 and 2 correspond to the solvent and polymer molecules respectively. Equation (6) is commonly used to predict the entropy of mixing polymer-solvent or polymer-polymer molecules. It is sometimes beneficial to express equation (6) on a volume basis as shown in equation 7:

$$\Delta S_{mix} = -R(V_1+V_2)\left[\frac{\phi_1}{V_1}\ln\phi_1 + \frac{\phi_2}{V_2}\ln\phi_2\right] \qquad \text{(Eq. 7)}$$

where V_1 and V_2 represent the molar volumes of their respective components. Knowing that molar volume is proportional to molecular weight, equation (7) illustrates that ΔS_{mix} decreases as molecular weight increases. In the case of infinitely high molecular weight, the entropy of mixing is negligible. Hence, for polymer blends, the change in the entropy of mixing is very small and the controlling factor leading to a negative ΔG_{mix} or miscibility is the enthalpy of mixing, ΔH_{mix} (23).

Combining equations 1, 2 and 7 gives equation 8 for Gibb's free energy of mixing:

$$\Delta G_{mix} = (V_1+V_2)B\phi_1\phi_2 + RTV \frac{\phi_1}{V_1} \ln\phi_1 + \frac{\phi_2}{V_2} \ln\phi_2$$

enthalpy (Interactions) entropy (randomness) (Eq. 8)

Owing to the logarithmic terms, the entropy part of equation 8 is always negative thus favoring miscibility. However, depending on the sign of B, the enthalpy part may or may not favor miscibility.

c. Solubility Parameter

For relatively non-polar components, the interaction parameter B can be estimated from the solubility parameters of the two components (24,25):

$$B = (\delta_1 - \delta_2)^2 \quad \text{(Eq. 9)}$$

The solubility parameter (δ) is defined as the square root of the cohesive energy density (CED) or the heat of vaporization per unit volume:

$$\delta = \left(\frac{E_{vap}}{V}\right)^{1/2} = (CED)^{1/2} \ (cal/cm^3)^{1/2} \quad \text{(Eq. 10)}$$

The solubility parameter is a measure of the strength of molecular attraction between molecules. Experimentally, solubility parameters are taken as equal to that of a solvent that will produce the greatest swelling of a lightly crosslinked version of the polymer or the highest intrinsic viscosity of a soluble polymer sample. A more convenient but often less reliable procedure relies on calculation of δ values rather than experimental assessment. The procedure, called group contribution employs the relationship

$$\delta = \rho\Sigma \frac{F_1}{M_0} \quad \text{(Eq. 11)}$$

where ρ is the density of the amorphous polymer at the solution temperature, M_o is the formula weight of the repeating unit, and ΣF_1 is the sum of all the molar attraction constants.

Since the solubility parameter is a measure of molecular attraction between molecules, and thermodynamics dictates that there is always a change of energy in a system when molecules are in contact with each other, it is logical that there should be a relationship between solubility parameter and enthalpy of mixing. This relationship is derived by combining equations 2 and 9, and it is called "Hildebrand Equation" (Eq. 12) (26).

$$\frac{\Delta H_{mix}}{V} = (\delta_1 - \delta_2)^2 \phi_1 \phi_2 \qquad \text{(Eq. 12)}$$

This relationship between solubility parameter and enthalpy indicates that the predicted value of ΔH_{mix} is always positive, and it approaches zero as δ_1 approaches δ_2. The Hildebrand solubility parameter treatment therefore favors phase separation rather than miscibility unless the enthalpy of mixing is much smaller than the entropic term. Despite this prediction, however, many polymer blends have been reported to be miscible (27,28). The miscibility is that of specific interactions between the two components. Such interactions between polymer 1 and polymer 2 indicate that the components prefer to interact with each other rather than with their own kind which results in a negative heat of mixing. In general the miscibility in polymer blends depends on (1) the chemical structures of the blending components, (2) the molecular weight and the molecular weight

distributions of the polymers, (3) the processing temperature, and (4) the method of sample preparation (29).

Properties of Polymeric Blends

The blending of polymers is an inexpensive way to alter the physical and mechanical properties of a material. Materials developed by blending can exhibit properties intermediate of those of the parent polymers or show improvement not only of one desired property but a balanced combination of several properties.

Miscible blends will exhibit a single glass transition (T_g) intermediate of that of its parent polymers. The actual value of the blend T_g is dependent on blend composition. A weighted average relationship between blend T_g and blend composition is expressed by the Flory-Fox equation given in equation 13,

$$\frac{1}{T_g} = \frac{W_1}{T_{g1}} + \frac{W_2}{T_{g2}} \qquad \text{(Eq. 13)}$$

where T_{g1} and W_1 are the glass transition temperature and weight fraction of the different components (30). Deviations from linearity can be described by the Gordon-Taylor equation which accounts for negative deviations by the introduction of an adjustable parameter k shown in equation 14 (31).

$$\frac{1}{T_g} = -\frac{W_1\ T_{g1} + W_2\ k\ T_{g2}}{W_1 + k\ W_2} \qquad \text{(Eq. 14)}$$

where T_{g1} and W_2 are identical to the parameters of T_{g1} and W_1 described in the Flory-Fox equation. The adjustable parameter, k, is

defined as the ratio of the difference in thermal expansion coefficient between the rubbery and glassy states of the blend components. Maximum deviation from linearity has been observed to occur when very strong interactions occur between the blend components. This type of deviation has been described by Kwei in equation 15 (32),

$$T_g = \frac{W_1 T_{g1} + W_2 k T_{g2}}{W_1 + k W_2} + q W_1 W_2 \qquad \text{(Eq. 15)}$$

where T_{g1} and W_1 represent the glass transition temperature and weight fraction of a given component, and k is an adjustable free volume coefficient. The new parameter, q, is an adjustable hydrogen bonding coefficient. Note, that at q=0 the Kwei model reduces to the Gordon-Taylor equation and at a k=1 the Gordon-Taylor equation reduces to the Flory-Fox equation. The generalized T_g-composition relationship expressed by equations 13-15 is illustrated in Figure 1.

How the modulus of both miscible and immiscible blends varies in relation to composition and temperature is illustrated in Figure 2. For both miscible and immiscible systems the modulus (log E') is plotted against temperature. In the case of miscible blends, (Figure 2A), the transition from a glassy to a rubbery material increases with respect to temperature as a larger amount of the high T_g material is added. Thus, by varying blend composition, materials with a wide range of T_g's can be engineered. On the other hand, immiscible blends (Figure 2B) show a modulus-temperature curve in which both materials exhibit softening transitions each corresponding to their respective

components. With partially miscible blends, transitions intermediate those for miscible and immiscible blends are observed. Figure 3A illustrates two partially miscible blends along with those of a miscible and an immiscible blend. Note that the partially miscible blend shows a gradual decrease in modulus over a relatively large temperature range. Certain applications may find this type of modulus behavior beneficial thus illustrating how a non-miscible system can be compatible and provide unique properties.

Figure 3B illustrates how the dissipation or damping factor, tan δ varies with temperature and composition. Tan δ is defined as the ratio of the work dissipated as heat to the maximum energy stored during one cycle of periodic deformation. Figure 3B illustrates that by controlling the extent of miscibility a material which is capable of dissipating energy over a wide range or at a specific temperature can be engineered.

The preceding discussion and figures illustrate that phase morphology and extent of miscibility are key parameters in determining mechanical properties. In systems which experience some degree of immiscibility the nature of the interface between the two phases is also a key parameter in determining mechanical properties (33). If the two polymers have a strong affinity for each other, but still show phase separation, the interfacial tension between the two polymers will be low in the melt state. This low interfacial tension will allow good interfacial adhesion in the solid state. However, if the interfacial tension is high in the melt state then poor interfacial adhesion will occur. In this case the discontinuous phase will not

contribute to the material properties.

Characterization Methods for Polymer Blends

Decisions as to whether a mixture is compatible or not are not always clearcut. They may depend in part on the particular method of examination. The sensitivity of the methods toward the dimensions of the phases of the components in the blend may also differ. Therefore different methods must be used to determine the extent of miscibility or compatibility of a polymer blend.

1) Visual observation

One of the simplest and fastest tests of miscibility is by visual observation. Blends which are miscible or compatible will be clear, transparent and self-supporting. Blends which are immiscible will be cloudy, and opaque. This method may be fast but it is also crude and by no means foolproof.

2) Microscopy

Techniques such as transmission electron microscope (TEM), scanning electron microscopy (SEM) and phase-contrast microscopy provide powerful tools for size, shape and orientation analysis. Due to the high resolution that can be achieved with SEM and TEM, these techniques have shown that several polymer blends that have been reported as miscible by other techniques were heterogeneous two-phase systems. Heterogeneity as revealed by microscopic techniques is only a relative property. For example, heterogeneity at the 50-100Å level has been detected in various reported by miscible blends (34).

3) Differential scanning calorimetry (DSC)

Differential scanning calorimetry is the most widely used method

for determining the glass transition temperatures of polymeric materials. The glass transition is defined as a discontinuity in the heat capacity Cp-vs-temperature curve. This discontinuity may also involve an enthalpy relaxation phenomena (22). Problems with distinguishing several sharp transitions may arise in the case where the T_g's of the parent polymers are close. In this case resolution is hindered and another technique will be needed to determine miscibility. DSC has the advantage of small sample requirements and relatively rapid analysis.

4) Dynamic mechanical thermal analysis

This technique has stricter sample requirements than DSC, but is often more sensitive. The dynamic mechanical measurement is nearly always that of a loss angle, tan δ, or the dynamic storage and loss modulus (E' or E"). This technique detects all motional transitions and can usually be obtained over a frequency or temperature range.

5) Fourier Transform Infrared Spectroscopy

If a blend is immiscible, the absorption spectrum of the blend will be the sum of those for the components. If a blend is miscible because of interaction between the two components, then differences will be noted in the spectrum of the blend. For example, hydrogen bonding involves a distinct shift of electron density from an electron-rich atom to between this atom and the proton. The shift in electron density lowers the vibrational transition energies associated with both old groups and considerable peak broadening is noted. For this reason FTIR is commonly used to study specific interactions.

6) Inverse Gas Chromatography IGC

Inverse gas chromatography is often used to study interactions between solvent and polymers. "Inverse" comes from the fact that the polymer, the test material, is the stationary phase and the solvent is the probe. IGC is capable of measuring thermodynamic parameters, such as χ, from a blend. Such parameters are calculated from retention volume data which is collected when a volatile probe is swept through a column containing a given polymer or polyblend. The retention mechanism is that of bulk adsorption of the probe on the surface of the polymer film. Therefore if strong interactions occur between two polymers of a polyblend less active sites will be available for interaction with the volital probe thus the probe will be swept through the column faster than expected from the rule-of-mixtures (35). In other words, differences in retention volumes of the individual polymers and that of the polyblend indicate the extent of polymer-polymer interactions occurring in a given blend. IGC is a rapid and inexpensive means of analyzing thermodynamic interactions between components of polyblends but problems may occur with column packing, where non-uniform polymer coating of the support material will result in deficient data. Since the retention volume of the probe depends on film thickness and the morphology of the system, two phase polymer systems, will in general give variable retention volumes thus unpredictable thermodynamic data.

Literature Cited

1) D. Fengel, G. Wegener, "Wood Chemistry, Ultrastructure, Reactions", Walter DeGruyter, Berlin, New York (1984).

2) A. C. Neish, "Monomeric Intermediates in the Biosynthesis of Lignin", In: Constitution and Biosynthesis of Lignin (Freudenberg, K. and Neish, A. C., Ed.), Springer-Verlag, Berlin, pp. 5-43 (1968).

3) K. V. Sarkanen, "Precursors and Their Polymerization". In: Lignins, Occurrence, Formation, Structure and Reactions (Sarkanen, K. V. and Ludwig, C. H., Eds.), Wiley-Intersci., New York, pp. 95-163 (1971).

4) K. V. Sarkanen and H. L. Hergert, "Classification and Distribution". In: Lignins, Occurrence, Formation, Structure and Reactions (Sarkanen, K. V. and Ludwig, C. H., Eds.), Wiley-Intersci., New York, pp. 43-94 (1971).

5) H. Grisebach, Naturwissenschaften 64, pp. 619-625 (1977).

6) G. G. Gross, "Biosynthesis of Lignin and Related Monomers". In: The Structure, Biosynthesis and Degradation of Wood. Recent Adv. in Phytochem. 11 (Loewus, F. A. and Runeckles, V. C., Eds.), Plenum Press, New York, pp. 141-184 (1977).

7) G. G. Gross, "Recent Advances in the Chemistry and Biochemistry of Lignin". In: Biochemistry of Plant Phenolics. Recent Adv. in Phytochem. 12 (Swain, T., Harborne, J. B. and Van Sumere, C. F., Eds.), Plenum Press, New York, pp. 177-220.

8) H. L. Chum, S. K. Parker, D. A. Feinberg, J. D. Wright, P. A. Rice, S. A. Sinclair, and W. G. Glasser. 1985. The Economic Contribution of Lignins to Ethanol Production from Biomass. SERI/TR 231-2488, pg. 1-86.

9) S. Y. Lin, 1983, "Lignin Utilization: Potential and Challenge", Progress in Biomass Conversion, Vol. 4, NY: Academic Press, p. 32.

10) Ibid, p. 33.

11) W. G. Glasser, Forest Prod. J., 31(3), 24 (1981).

12) Kringstad, K., In: Future Sources of Organic Raw Materials -CHEMRAWN I, (St. Pierre and Brown, Eds.), Pergamon Press, New York, pp. 627 (1980).

13) T. G. Rials, and W. G. Glasser, Holzforschung. 38, pp. 191-199 (1984).

14) T. G. Rials, and W. G. Glasser, Holzforschung, 38, pp. 263-269 (1984).

15) V. P. Saraf, W. G. Glasser, and G. L. Wilkes, J. Appl. Polym. Sci., Vol. 30, pp. 3809-3823 (1985).

16) P. C. Muller, S. S. Kelley, and W. G. Glasser, J. Adhesion. Vol. 17, pp. 185-206 (1984).

17) R. G. C. Arridge, "Mechanics of Polymers". Clarendon Press, Oxford (1975).

18) J. F. Kenney, "An Approach to New Polymeric Materials Via Blocks, Grafts and Blends". In: Polymer Alloys (D. K. Klempner and K. C. Frisch, Eds.), Plenum Press, New York, pp. 19-38 (1977).

19) "Polymer Blends", Polym. Eng. Sci., 22 (2) (1982).

20) G. Scatchard, Chem. Rev. 8, 321 (1931).

21) J. H. Hildebrand, J. M. Pravsnitz, and R. L. Scott, "Regular and Related Solutions". Van Nostrand Reinhold, New York, 1970.

22) A. Rudin, "The Elements of Polymer Science and Engineering", Academic Press, New York, N. Y., pp. 428-442 (1982).

23) G. Ronca, and T. P. Russell, Macromolecules (18), pp. 665-670 (1985).

24) T. Inoue, T. Ougizawa, O. Yasuda, and K. Miyasaka, Macromolecules (18), pp. 57-63 (1985).

25) H. W. Kammer, and J. Piglowski, "Adhesion Between Polymers". In: Polymer Blends II (M. Kryszewski and A. Galeski, Eds.), Plenum Press, New York, pp. 19-34 (1984).

26) O. Olabisi, J. Chem. Education, 58(11), pp. 944 (1981).

27) R. Kuhn, "Characterization of Polyblends". In: Polymer Alloys III (D. Klempner and K. C. Frisch, Eds.), Plenum Press, New York, pp. 45-58 (1983).

28) L. P. McMaster, Macromolecules, 6, 760 (1973).

29) J. W. Barlow and D. R. Paul, Polym. Eng. Sci., 21(15), p. 985 (1981).

30) T. G. Fox, Bull. Am. Phys. Soc., 1, p. 123 (1956).

31) M. Gordon and J. S. Taylor, J. Appl. Chem., 2, p. 493 (1952).

32) T. K. Kwei, J. Appl. Polym. Sci., 22, pp. 307-313 (1984).

33) D. R. Paul, Org. Coat. Prepr., 50, 187th National ACS Meeting, St. Louis (1984).

34) R. A. Orwell, Rubber Chemistry and Technology 50, p. 451 (1977).

35) D. P. Sheehy, Ph.D. Dissertation, VPI & SU (1984).

List of Figures

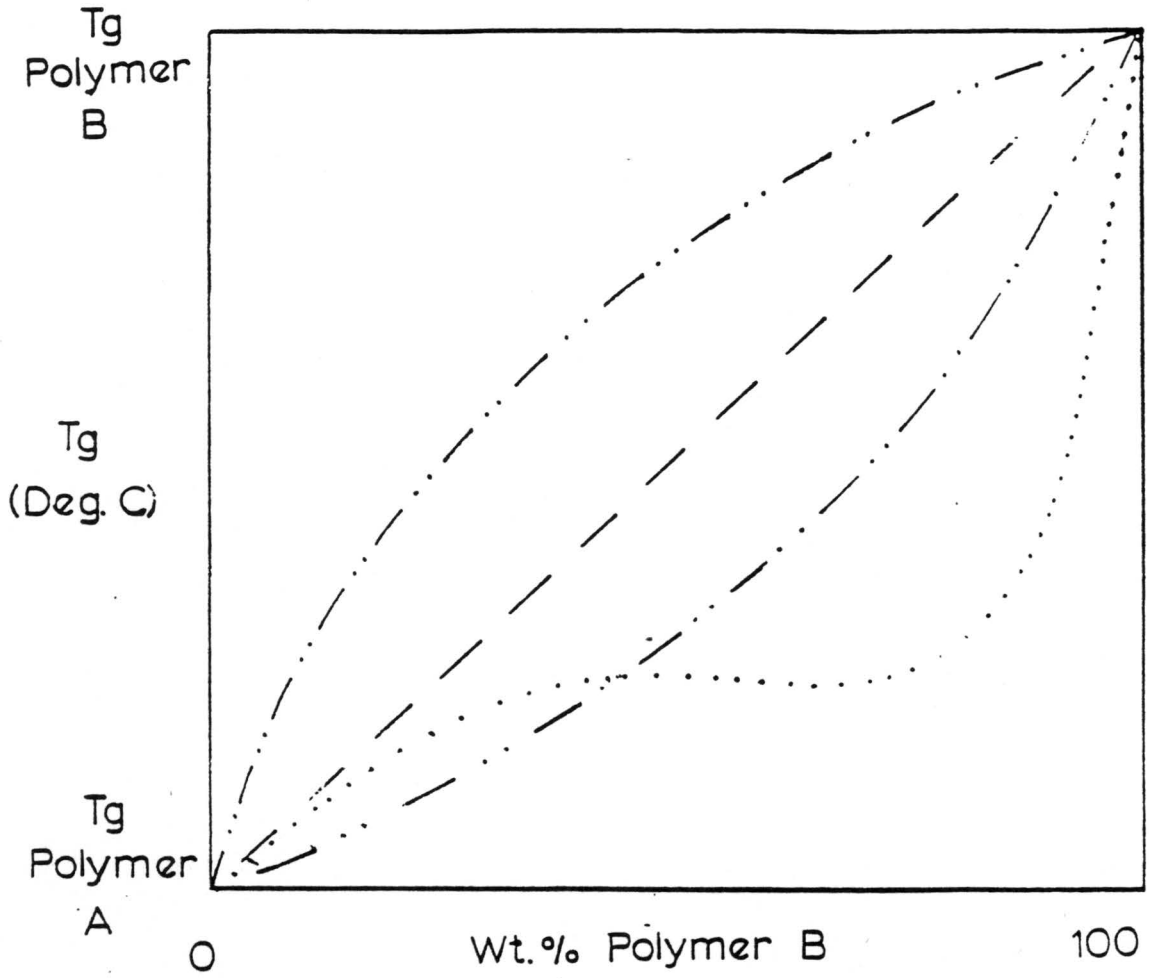

Figure 1. Theoretical changes in blend T_g as polymer B is added to polymer A.

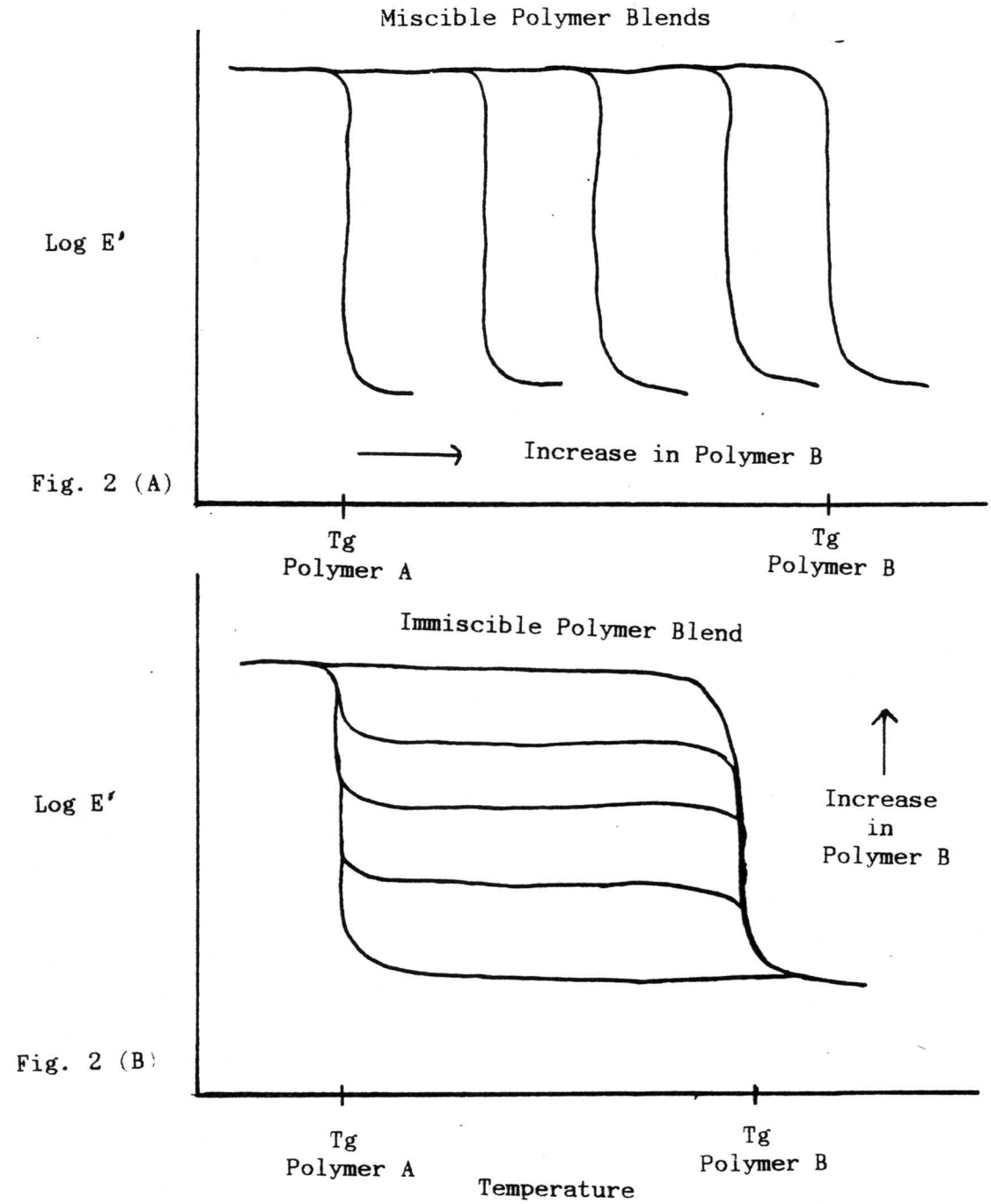

Fig. 2 (A)

Fig. 2 (B)

Figure 2A and B. Generalized changes in log storage modulus (E') as polymer B is added to polymer A.

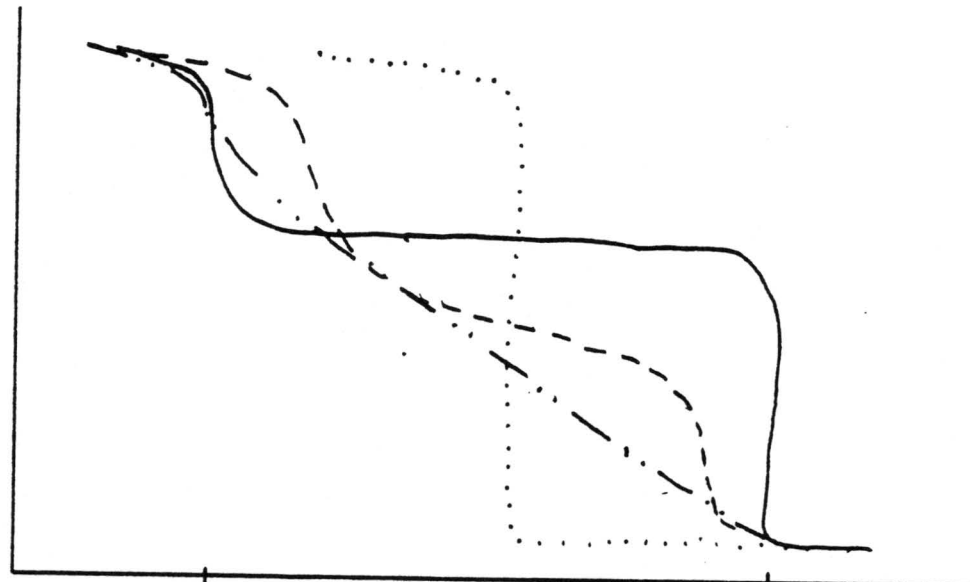

Fig. 3 (A)

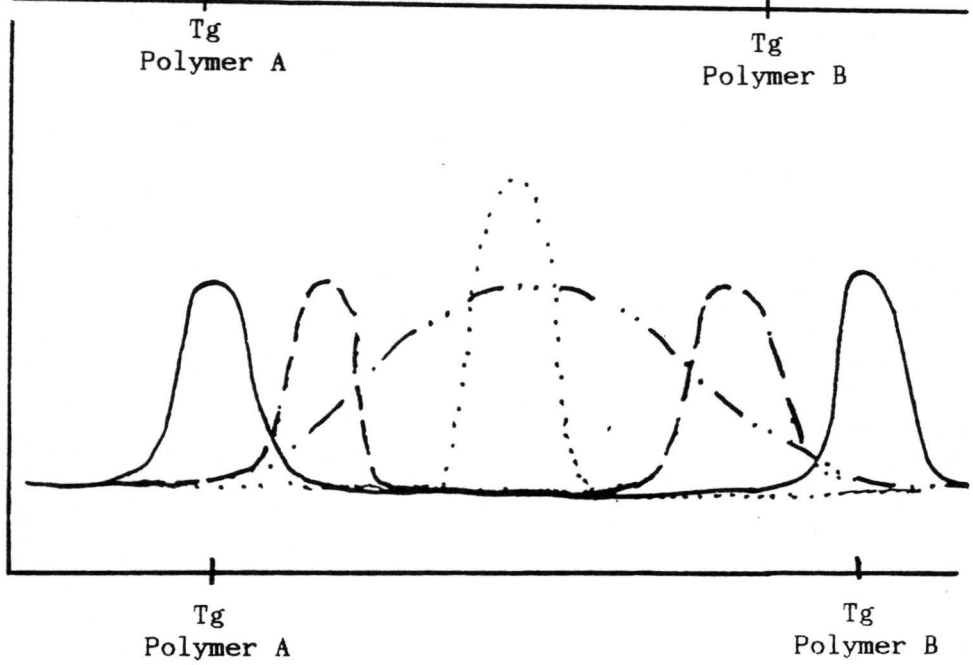

Fig.3 (B)

Figure 3A. Generalized changes in log storage modulus (E') when considering various degrees of miscibility.

3B. Generalized effects of various degrees of miscibility on tan δ.

CHAPTER 1. PROPERTIES AND MORPHOLOGY OF HYDROXYPROPYL LIGNIN/POLY(METHYL METHACRYLATE) BLENDS PREPARED BY SOLUTION CASTING AND INJECTION MOLDING

(ABSTRACT)

Polymer blends consisting of hydroxypropyl lignin (HPL) and poly(methyl methacrylate) (PMMA) were prepared by injection molding and solution casting with THF (a hydrogen bonding solvent) and chloroform (a non-hydrogen bonding solvent). Blend morphology and material properties were discussed in terms of HPL content, HPL molecular weight and method of preparation.

Blends of PMMA and various molecular weight HPL's formed two phase system. SEM results showed that solution cast blends formed distinct domains whereas injection molding creates a blend in which the HPL is found in striations of various widths. The interphase between the domains and matrix of the blends varied with respect to the method of preparation. Solution cast blends showed domains that were "pulled away" from the matrix however the injection molded blends showed HPL striations that were closely associated with the matrix. This difference was believed to be due to the fast time of vitrification experienced by the injection molded samples.

Both DSC and DMTA T_g values for blends prepared by injection molding followed the same trends shown by the Flory-Fox equation thus possibly indicating some degree of miscibility. However even the highly phase separated solution cast blends showed single T_g's at all HPL contents. Therefore, analysis of the T_g data is unclear since the T_g values are believed to be effected by transitional smearing.

The addition of HPL to PMMA was found to cause an increase in modulus and a decrease in ultimate properties and tensile strength. However blends prepared by injection molding had consistently better material properties than those prepared by solution casting.

Introduction

Polymer blends have become a very important subject for scientific investigation because of their growing commercial acceptance. Blending is seen as an inexpensive method for the modification of polymer properties. The modification of polymer properties due to the blending of two polymers, is governed by the miscibility or compatibility of the two polymers. Two polymers are termed miscible if they form a single, homogeneous phase and intimate mixing is achieved on a molecular scale. On the other hand compatibility, being more of a commercial term, indicates the usefulness of a blend. Thus, immiscible blends do in certain cases exhibit good mechanical properties and are said to be mechanically compatible (1). Mechanical compatibility in immiscible blends is generally related to good interfacial adhesion between the phases of the blend constituents. A number of immiscible, but compatible blends have drawn considerable commercial interest in recent years. These include, bisphenol-A polycarbonate/poly(butylene terephthalate) (PC/PBT) (2), poly(vinyl chloride)/acrylonitrile-butadiene-styrene terpolymer (PVC/ABS) (3,4), poly(vinyl chloride)/poly(methyl methacrylate) (PVC/PMMA) blends (2). The last mentioned blend, PVC/PMMA, is a good example of how blending can be used to improve a polymer's properties. PVC/PMMA blends combine the good flammability resistance of PVC and the higher T_g of PMMA relative to PVC. The blends exhibit higher notched impact strength than either of the blend components. PMMA also improves the thermoforming characteristics of PVC. The combination of these improved properties has allowed PVC/PMMA blends to be used in specific

applications such as seat backs, aircraft interior components and industrial wall paneling (2).

In miscible systems, specific interactions that occur between components will increase the overall entanglement of the network structure. Thus, miscible blends have the assurance of mechanical compatibility. One of the most commonly known and commercially interesting miscible blends is that of polystyrene and poly(2,6-Dimethyl-1,4 Phenylene oxide)(PS/PPO) (5). This blend is miscible at any composition range and hence blends of any desirable T_g can be obtained by simply varying the composition of the constituents. Miscibility between PS and PPO was reported to be due to (among other things) specific interaction of the phenylene group of PPO and the phenyl group of PS (6).

Two polymers may form an immiscible blend, a miscible blend, or an intermediate. Since the material properties of a polymer blend vary with the degree of miscibility, an understanding of the parameters affecting miscibility must be established before polymer blends with unique properties can be engineered. (A more exhaustible treatment of this basis is found in the introduction; the following represents a brief summary).

The basic equation describing the state of miscibility of a two component system is given by:

$$\Delta G = \Delta H - T\Delta S \qquad \text{(Eq. 1)}$$

where ΔG_{mix} = Gibb's free energy of mixing

ΔH_{mix} = Enthalpy of mixing

ΔS_{mix} = Entropy of mixing

T = temperature

In order for a mixture to be miscible ΔG_{mix} must be negative (7). Thus, miscibility of a two component mixture depends on the magnitude and the sign of ΔH_{mix} and ΔS_{mix}. When dealing with polymer blends the magnitude and sign of ΔH_{mix} and ΔS_{mix} are governed by three parameters: 1) solubility parameters, 2) molecular weight of the polymers, and 3) specific interactions between the polymers.

The solubility parameter is a measure of the cohesion of the material or the strength of molecular attraction between molecules. The importance of the solubility parameters and specific interactions between the polymers is illustrated by the following. ΔH_{mix} values are the net result of breaking solvent-polymer (1-2)(1-3) contacts and making polymer-polymer (2-3) contacts thus the more polymer-polymer (2-3) interactions that occur the more exothermic ΔH_{mix}. This in turn would result in a more negative ΔG_{mix}.

The effects of molecular weight on miscibility are revealed by equation 1 and the Flory-Huggins theory. Equation 1 points out that any measure that increases the entropy of mixing (ΔS_{mix}) will favor a more negative ΔG_{mix}. The Flory-Huggin's theory indicates that the entropy gained on mixing a polymer is inversely related to the number average size (7). Thus, holding other factors constant, a particular polymer mixture can be made more miscible by reducing the molecular weight of one or both components.

This study continues on-going research at Virginia Tech dealing with engineering plastics from lignin. This particular contribution

involves the blending of HPL with PMMA. Emphasis will be placed on the effects of molecular weight and specific interactions between polymers. The primary objectives of this study are as follows:

1) To blend poly(methyl methacrylate) (PMMA) with hydroxypropyl lignin (HPL) and describe the state of miscibility and the material properties of the resulting materials.

2) To introduce molecular weight of HPL as a variable and determine its effect on both miscibility and material properties. This is to involve fractionating HPL by a solvent - non-solvent technique whereby the resulting molecular weight fractions will be incorporated into polyblends.

3) To compare three preparation techniques; a) solution casting with a hydrogen bonding solvent (THF), b) solution casting with a non-hydrogen bonding solvent (chloroform), and c) injection molding in terms of film morphology, thermal mechanical and mechanial properties.

Materials and Methods

I. Materials:

1) Kraft lignin

A commercially available kraft lignin (Indulin from Westvaco Corp., Charleston, South Carolina) was used in this study. This lignin was isolated from the spent pulp liquor of a pine based pulping process, and it was purified by reprecipitation from alkaline solution with acid.

2) Hydroxypropyl lignin

Kraft lignin was reacted with propylene oxide under basic

conditions in toluene. This procedure has been described previously (10). The reaction product was isolated by a liquid-liquid extraction with hexane and acetonitrile. The hydroxpropylated lignin derivative had a hydroxyl content of 6.5% (by titration). The H-NMR spectrum of the acetylated derivative had 16.0% aromatic protons (range 2), 8.5% aliphatic carbon-linked protons (range 3-4), 35.0% CH_2 and methoxy protons (range 5), 20.0% aliphatic acetoxy protons (range 6) and 21.0% methyl protons (range 8). The glass transition temperature of the hydroxypropyl lignin was 63.5°C (by DSC with a heating rate of 10°C/min).

3) Poly(methyl methacrylate)

A commercially available atactic poly(methyl methacrylate) (PMMA) having a glass transition temperature of 110°C and an intrinsic viscosity of 1.4 as reported by Polyscience Inc.

II. Methods:

1) Fractionation of HPL

Fractionation of hydroxypropyl lignin was carried out by differential solubility of macromolecules. Initially, 150 g of HPL was dissolved in 7500 mL of acetone, giving a 2% weight to volume solution. To this solution 9375 mL of a non-solvent, hexane, was added, giving a solvent to non-solvent ratio of 1 to 1.25. The material remaining in solution was isolated by solvent evaporation (fraction #1). The material that precipitated was dried, reweighed and dissolved in enough acetone to give a 2% solution. Once again a non-solvent, hexane, was added but a ratio of 1 to 0.75 solvent to non-solvent was used. The material remaining in solution was isolated

in the same manner and labeled fraction #2. The precipitated material was isolated and the process was repeated using a solvent to non-solvent ratio of 1 to 0.5. The material remaining in solution after this stage was isolated and labeled fraction #3. The precipitated material was labeled fraction #4.

2) Solution cast blends

Separate 10% (w/w) solutions of each component were prepared using tetrahydrofuran and chloroform as solvents. The solutions were mixed together, and they were allowed to stir at room temperature overnight. This solution was poured into Teflon molds and the solvent was allowed to evaporate slowly at room temperature for 2 days. The resulting films were dried in a vacuum oven at 70°C for a week and then stored in a dessicator containing P_2O_5.

3) Injection Molding

The proper weight percent of each polymer component was weighed out separately and mixed by mortar and pestle before being placed in the injection molder. A "Mini-Max Molder" by Custom Scientific Instruments was used. Approximately 0.5 g of material was placed in the stator cup heater, which was set at 230°C. The sample was stirred for 1 min and then injection molded into a dog bone mold.

4) Characterization of HPL Fractions

a) Molecular weight determination by GPC

Number average ($\overline{M}_n$) and weight average ($\overline{M}_w$) molecular weights were determined by gel permeation chromatography (GPC) in tetrahydrofuran or DMF/LiBr on ALTEX (Beckman) columns packed with polystyrene divinyl benzene resin of gel sizes 500A, 1000A, 10,000A and 100,000A.

b) Molecular weight determination by VPO

Number average molecular weight was also determined by vapor pressure osmometry (VPO) using a Knauer Dampfdruck instrument. Initially a calibration curve was produced using benzil, a standard with a molecular weight of 210.22. Dilutions were made between 0.02 and 0.1 molality. The change in temperature measured by osmometry was plotted against the concentration, and the Y intercept was determined. The experimental data was plotted as the instrument reading/$Cgkg^{-1}$ -vs-$Cgkg^{-1}$. This same procedure was used with HPL solutions and a comparison of the Y-intercept produced by the model compound of known molecular weight to the Y-intercept of HPL allowed the determination of the HPL molecular weight.

5) Determination of Physical Properties

a) Differential Scanning Calorimetry (DSC)

DSC scans were run on samples weighing roughly 20 mg with a Perkin-Elmer DSC-4 instrument. Scans were started at a temperature of 15°C and heated at a rate of 10°C to a final temperature of 150°, quenched and rescanned under the same conditions. All scans were run under a dry nitrogen atmosphere. The glass transition temperature (T_g) was defined as one-half the total change in heat capacity (C_p) occurring over the transition region. This method was used for both starting materials, including all fractions and the polyblends.

b) Dynamic Thermal Mechanical Analysis DMTA

Dynamic thermal mechanical properties of the polyblends were determined using a Polymer Laboratories DMTA instrument. Sample dimensions for the extruded dog bones were roughly 3 mm in width,

1.5 mm thick, and 10 mm in length. Dimensions for the solvent cast films varied so to keep the calibration constant log k between 3.5 and 4 while running single cantilever beam mode with a free length of 1 mm. All samples were run at a heating rate of 5°C per min and a frequency of 1 Hz.

c) Stress-strain

The tensile properties were measured at room temperature using an Instron table model TM-M at a cross head speed of 1 mm/min. All samples had gage length of 13 mm and solution cast films had widths of 2.5 mm and variable thickness. The data reported are the average of at least seven samples. The Young's modulus was obtained from the tangent of the initial slope of the force vs. elongation curve.

d) Scanning Electron Microscopy (SEM)

Fractured surfaces were observed using an AMR 900 scanning electron microscope. In order to prevent charging the samples were coated with 100A of Gold-palladium. Samples were then observed at magnifications ranging from 500 x to 5000 x.

e) Stereology

Sterology refers to the quantitative characterization of microstructures. This procedure involves the application of geometrical-statistical techniques and equations which relate measurements upon two-dimensional sections to three-dimensional structural quantities (11). In this case two-dimensional SEM micrographs were analyzed in order to describe the three-dimensional structures of polyblend domains. The statistical sampling of the micro-structure involves measurements of section images upon which

grids or test lines are superimposed. Measured quantities such as point fractions, intercept and feature counts are then related to structural quantities such as volume fraction (or volume percentage), surface area per unit volume, diameters, etc.

Results and Discussion

Fractionation

Fractionation of hydroxypropylated lignin was performed in order to generate different molecular weight fractions of more uniform polydispersity. The fractions were isolated by varying the ratio of solvent (acetone) to non-solvent (hexane). At a low acetone/hexane ratio the large amount of hexane causes only the most soluble, low molecular weight, material to remain in solution. Sequentially higher molecular weight fractions were isolated by increasing the acetone to hexane ratio. The final precipitant had the highest molecular weight material. A summary of the molecular weight data of the fractions isolated is shown in Table 1.

The percent material collected for each fraction is given in column 3 of Table 1. It was found that fractions 1 and 4 contained 60% of the total material collected, whereas fractions 2 and 3 represented only 16 and 9%, respectively. The large amount of material found in fractions 1 and 4 indicates that these fractions would be more polydispersed than fractions 2 and 3. In order to obtain a more uniform fractionation in terms of percent material in each fraction, the acetone hexane ratios for fractions 1 and 2 would need to be decreased. This would allow more material to be collected

in fraction 3. Due to the low yield of fraction 3 only three fractions - 1, 2 and 4 or low, medium and high - will be employed for blend preparation.

Molecular weights were determined by GPC, GPC-viscosity and by VPO. Data collected by GPC can be found in columns 5, 6 and 7 of Table 1. It should be noted that the GPC columns were calibrated in THF with polystyrene molecular weight standards as well as with lignin-like model compounds. Since problems were encountered with the monitoring of polystyrene with a UV_{280} detector, a calibration curve was constructed on the basis of the elution behavior of lignin model compounds in the low molecular weight region and of polystyrene standards in the upper molecular weight range (12). Column 5 of Table 1 shows the GPC for HPL fractions that were analyzed in THF. This data shows an expected overall trend of both $\overline{M}n$ and $\overline{M}w$ increasing in value with increasing acetone/hexane ratio. When comparing this data with that of fractions run in DMF-LiBr, found in column 7, the same overall trend of $\overline{M}n$ and $\overline{M}w$ increasing with acetone/hexane ratio is observed. However, the DMF-LiBr samples are 3 to 10 times those found with THF. Past research has indicated similar difficulties in determining molecular weights for lignin and lignin derivatives (13,14,15). Most of the problems involved in lignin molecular weight determination center around an association phenomenon which lignin is believed to be involved in and the reliability of molecular weight standards used to calibrate the GPC columns (16). Thus, in order to help clarify this problem another method of molecular weight determination was utilized.

This system used THF as a solvent and GPC columns similar to those used before. However instead of a UV detector molecular weights were directly calculated based on viscosity measurements. Column 6 of Table 1 contains the $\overline{M}_n$ and $\overline{M}_w$ data obtained by this method. The same trend of increasing $\overline{M}_n$ and $\overline{M}_w$ with increasing acetone/hexane ratio was found. The actual $\overline{M}_n$ and $\overline{M}_w$ values more closely follow those found with DMF-LiBr but sizable discrepancies can be seen with the higher molecular weight fractions. These discrepancies with the high molecular weight fractions can be explained by the lack of reliable molecular weight standards for the high molecular weight portion of a calibration curve (14,15,16). Like the GPC and viscosity data the $\overline{M}n$ data collected by VPO also showed the trend of increasing $\overline{M}n$ value with increasing acetone/hexane ratio. Therefore all of the molecular weight techniques employed showed the same overall trend, that being, the fractions do increase in molecular weight from fraction 1 to fraction 4. However discrepancies do exist in the actual values of both $\overline{M}n$ and $\overline{M}w$.

Glass transition temperatures for the fractions are listed in column 4 of Table 1. The data shows, in accordance with Fox-Flory, that the T_g of the fractions increases with molecular weight. This relationship is shown in Figure 1 where T_g data and GPC (THF) molecular weight data from this study along with that produced by Kelley (15) was found to follow the Fox-Flory equation (Eq. 2) (17).

$$T_g = T_{gw} - \frac{k}{M_n} \qquad \text{(Eq. 2)}$$

where T_g = the glass transition temperature

T_g = the glass transition temperature at infinite molecular weight

k = constant related to the excess free volume per chain end

M = molecular weight

An excellent agreement was established between the experimental data obtained with the HPL fractions and the model (i.e. $R^2 = 0.95$). Glass transition temperature at infinite molecular weight is suggested as being 143°C, and k was found to be -100,022.

Due to the discrepancies in the molecular weight values obtained from the various methods used in this study and the fact that the objective of this study was not to answer the problem of lignin molecular weights the molecular weight data which fit the Fox-Flory equation, that being the GPC (THF) data found in column 5 of Table 1 will be assumed for the remainder of this paper.

The chemical composition of the HPL fractions was investigated by Kelley (15). He found that the chemical properties, as determined by H-NMR and UV of the fractions varied slightly with molecular weight. For example, the hydroxyl content of the fractions was found to decrease as the molecular weight of the HPL increased. Overall, it was, however, concluded that the apparent differences in chemical structure with increased molecular weight were not substantial.

Blend Structure

Figure 2 shows some typical SEM photomicrographs of PMMA and PMMA/HPL blends. Figure A shows that pure PMMA can be characterized by rather regular parabolic structures with lines radiating from an

area near the focus. This photomicrograph is of extruded PMMA, however photomicrographs of PMMA cast from THF and chloroform showed identical structures. Figures B, C are of blends consisting of 25% unfractionated HPL and 75% PMMA casted from THF and chloroform, respectively. It is clear from these photomicrographs that unfractionated HPL and PMMA form multiphase immiscible systems (when cast from THF and chloroform). The same immiscible state was observed for solution cast blends made with each molecular weight fraction at all HPL levels. In other words, molecular weight of the HPL did not affect extent of miscibility.

Figure 2D shows an extruded blend of HPL and PMMA. Note, that the domains seen in Figures 2B, C are not present in the extruded blends. In order to distinguish the morphology of the extruded blends an etching procedure was performed. Methanol, which is a solvent for HPL and a non-solvent for PMMA was repeatedly wiped across the surface of the blend in order to remove a portion of the HPL. The resulting material is seen in Figure 2E. Even though the material is somewhat distorted it can still be seen that the HPL was removed from long narrow striations, indicating that phase separation did occur with the injection molded blends. However it is quite evident from Figures 2B, C and D that substantial differences exist in terms of blend morphology between solution casting and injection molding. These different morphologies are believed to result from the differences in the time of vitrification between the two methods. Injection molding, which would have a fast time of vitrification when compared to

solution casting, would tend to "lock" the two blend components in a random entangled state or a state very similar to that of a highly mixed melt. By contrast, solution casting with a longer time of vitrification would allow the two blend components to separate in a more ordered manner thus resulting in distinct domains.

Figures 2B, C and D also illustrate differences in the state of the interphase between HPL and PMMA. Figures 2B and C show that for solution cast blends the domains are pulled away from the matrix. From this kind of interphase it could be assumed that at room temperature, little or no interaction occurs between the two phases. The same interphacial conditions were observed for all solution cast blends regardless of HPL molecular weight or load level. However Figure 2D shows that the injection molded blends have a closer associated interphase. The discontinuous polymer (HPL) does not show visible signs of being "pulled away" from the matrix as was observed with the solution cast blends. This once again is believed to be associated with the fast time of vitrification for injection molding. This type of closely associated interphase does present the possibility of polymer-polymer interactions. Therefore it is believed that the blend produced by injection molding would have better material properties than those produced by solution casting.

In order to more fully describe the morphologies of both solution cast and injection molded blends, stereology was employed. Stereology, which is a geometrical-statistical technique for characterizing three-dimensional structures from two-dimensional sections, was used

to calculate domain size and the percent volume that the domains occupied. For the solution cast blends the stereological procedure indicated that the blends containing 5% HPL had domains that occupied 5% (± 05%) of the blend volume; and the same was true for the 25% and 40% solution cast blends. No significant trends or differences were seen between blends with HPL of different molecular weight. Analysis of the injection molded blends was made difficult due to the lack of distinct domains. However an attempt was made to measure the width of the striations that were made visible upon etching. This data is presented in Figure 3 along with the domain sizes for comparative purposes.

Figure 3 shows how domain size varies in relation to method of preparation, molecular weight of HPL, and volume fraction of HPL. Domain size was found to increase with both increasing amount of HPL and increasing molecular weight of HPL. This increase in domain size was observed with both solvents though the slope and magnitude of the curves were different for each solvent. The curves indicate that the chloroform films had consistently greater domain dimensions than those of THF films. Whereas the injection molded blends showed striation widths that were smaller than the THF domains and these striation widths remained fairly constant with respect to HPL molecular weight. This is clearly seen with the chloroform data in Figure 3.

This difference in domain size is, thus far, the first difference noticed between chloroform and THF in this study. It was hoped that since the solubility parameters of the two solvents are almost

identical (chloroform δ = 9.3, THF δ = 9.1) that the difference in hydrogen bonding potential would produce different degrees of miscibility. Apparently with HPL/PMMA blends such solvent effects are not large enough to affect the nature of the polymer-polymer interphase however solvent was found to cause domain size differences.

Thermal Properties

A) Differential Scanning Calorimetry (DSC)

DSC thermograms of polymer blends are sometimes complicated by the two phase microstructure which can exist. In the case where two polymers are totally immiscible a DSC thermogram will show two T_g's, one for each polymer. On the other hand, if two polymers are miscible the result will be a single T_g in between that of the two parent polymers. The complexity of DSC thermograms is greatly increased when considering the fact that various degrees of miscibility can exist (18). For example, a 25/75 partially miscible blend of poly(methyl methacrylate) (T_g 100°C) and bisphenol-A polycarbonate (T_g 150°C) produced a DSC thermogram with two T_g's one at 115° and a second at 142°C (19). DSC scans are further complicated when the blend components have T_g's that lie within 20° or less of each other. In this case the individual transitions are difficult to distinguish due to what is called "transitional smearing". Transitional smearing is simply the overlapping of two T_g's to produce a single broad T_g.

If we consider the point where the DSC curve deviates from the baseline as T_{gi} and label T_{gf} as the point after the endotherm where the DSC curve returns to the baseline then ΔT_g can be defined as

$$\Delta T_g = T_{gf} - T_{gi} \qquad \text{(Eq. 3)}$$

A sharp transition ($\Delta T_g < 15^oC$) is typical of a homogeneous polymer material. A broad transition on the other hand, suggests a somewhat less than homogeneous blend (20). MacKnight has discussed broad transitions in terms of blend compatibility. He described compatible blends as those exhibiting a sharp transition and a less compatible blend as those exhibiting a wider, broader transition. With the extreme case being a totally incompatible material which would show two separate transitions, signifying little attraction of one component for another (21).

Figure 4 shows what was found to be a typical DSC scan for a solution cast and an injection molded HPL/PMMA blend. The upper curve shows a small endotherm at 63°C which relates to the HPL component and a second endotherm at 104°C which relates to PMMA. These endotherms are related to the phenomenon of enthalpy relaxation. Enthalpy relaxation occurs when a polymer is cooled from the melt. The rapid rise in viscosity that occurs as the polymer approaches T_g causes the polymer chain to freeze into non-equilibrium conformations leaving an excess free volume quenched into the system (22).

The lower scan shown in Figure 4 shows that after heating the blend above the T_g of PMMA quenching and rescanning the thermal history has been erased. Thus the two endotherms that were associated with the enthalpy relaxation of the respective polymers have been replaced with a single broad T_g. Considering the results from the SEM analysis (which indicated that the solution cast blends of HPL/PMMA

were immiscible and showed little or no signs of interactions between the two phases) the presence of this single T_g is not considered an indication of miscibility. Rather, this broad T_g, which in the case of the low molecular weight HPL spans a 90 degree range, is believed to be the result of transitional smearing.

Typically miscible blends will follow equations such as Flory-Fox:

$$\frac{1}{T_g} = \frac{W_1}{T_{g_1}} + \frac{W_2}{T_{g_2}} \qquad \text{(Eq. 4)}$$

where $W_{1,2}$ = weight fraction of polymer 1 and 2, and

$T_{g1,2}$ = glass transition of polymer 1 and 2

which results in blend T_g's that are weighted averages of the parent polymers. Figures 5A, B, C and D show the HPL/PMMA blend T_g's that were calculated using the Flory-Fox equation along with the actual experimental data for blends made by solution casting and injection molding. Figure 5A contains T_g data of blends made with unfractionated HPL and PMMA. The Flory-Fox equation predicted that the T_g would gradually drop from 110°C to 87°C as the HPL content of the blends change from 0% to 40%. The T_g values for the injection molded samples were found to follow a similar gradual drop in T_g; however the actual values for the injection molded blends are 5 to 10°C higher than those predicted by the Flory-Fox equation. By contrast, the solution cast blends did not follow the same gradual drop in T_g. Blends casted from THF did show a slight decrease in T_g with increasing HPL content; however the total change was only 3°C

compared to a 23°C change shown by the Flory-Fox equation for the same change in HPL content. T_g data from blends cast with chloroform also showed an overall decrease in T_g with increasing HPL content. At 25% HPL, however an increase in blend T_g was observed. Figures 5B and C once again show that the injection molded blends have T_g's that follow the same trends shown by the Flory-Fox model. In the case of blends made with HPL of low molecular weight, shown in Figure 5B, the Flory-Fox equation predicts a fairly sharp decrease in blend T_g, from 110°C for pure PMMA to 51° for a blend containing 40% HPL. Injection molded blends did not reflect as sharp a decrease in blend T_g, its T_g dropped only from 110°C for pure PMMA to 71°C for a blend containing 40% HPL. However solution cast blends with both chloroform and THF showed decreases in T^g's at 5% HPL content but remained fairly constant with additional increases in HPL content. Likewise the solution casted blends made with HPL of medium molecular weight, shown in Figure 5C, did not follow the same trends observed by the model and injection molded blends. In this case the injection molded blends duplicated the trend of decreasing T_g with increase HPL content shown by the Flory-Fox model. The T_g values of the injection molded blends were 3°C higher than those predicted by the model at all HPL load levels. Figure 5D shows the T_g values for blends made with HPL of high molecular weight. The high molecular weight HPL had a T_g of 105°C therefore since the T_g of PMMA is 110°C the Flory-Fox model predicted a fairly straight line relationship between T_g and HPL content. This predicted relationship is once again reproduced by the

injection molded blends. Blends cast from chloroform also showed a fairly straight line relationship between blend T_g and HPL content however the T_g values are 20° lower than those shown by the model.

When analyzing the T_g data given in Figures 5A, B, C and D, it is important to remember that the SEM micrographs indicated that the solution cast blends where two phase immiscible systems despite the fact that single T_g's were noted for all blends regardless of the method of preparation, HPL molecular weight or HPL content. Therefore it is believed that many of the T_g's reported for the solution cast blends are the result of transitional smearing or more simply the overlapping of two T_g's. This transitional smearing could also explain some of the inconsistencies found in the solution cast T_g data. However from Figures 5A, B, C and D it is apparent that the injection molded samples show more consistency in terms of T_g-vs-HPL molecular weight and HPL content than was found with the solution cast blends. Injection molded samples were found to follow T_g values predicted from miscible blends according to the Flory-Fox equation. With almost perfect duplication occurring with blends containing an HPL of medium molecular weight. It was also observed that blends solution cast from THF produced T_g's that followed the model more closely than those from chloroform. This could be explained by the fact the THF being a hydrogen bonding solvent is more capable of disrupting association within the HPL macromolecule thus enabling the HPL to associate with PMMA.

b) Dynamic Mechanical Thermal Analysis (DMTA)

Thermal analysis by DSC indicated that HPL/PMMA blends produced a single broad T_g. This single T_g was not taken to be an indication of miscibility but rather a result of transitional smearing. In order to help clarify the nature of this transition another form of thermal analysis was employed, dynamic mechanical thermal analysis.

Figure 6 shows the temperature vs. tan δ and the temperature vs. storage modulus (log E') curves for PMMA. These spectra for pure PMMA are typical and have been described by numerous authors, though different frequencies may slightly change the spectra (23). The α or glass transition appears at 112° for the extruded sample, 108°C for the THF casted sample and 104° for the chloroform casted sample, as determined by the tan δ curve. The α transition, which is generally accepted to arise from rotation of the methyl ester side group is a broad shoulder in the tan δ spectrum centering around 20-50°C (24). The modulus curves for the extruded samples showed an initial log storage modulus of 9.75 this modulus remained relatively constant up to a temperature which correlates to the beginning of the α-transition in the tan δ curve. At this temperature the material experiences the onset of large scale molecular motion which is characteristics of the rubbery state. Thus the log storage modulus decreases to a value of 7.8. It should be pointed out that the modulus reading for the DMTA analysis is highly sensitive to the stability of the sample dimensions. Therefore when analyzing thermoplastic materials such as HPL/PMMA blends, especially thin films, the values for the log modulus are questionable. For this

reason the emphasis of this analysis will center on the tan δ data.

Figures 7A, B and C show the effects of increasing HPL content and of increasing molecular weight, on the shape of the log tan δ curve. Figure 7A shows that with the addition of 5% HPL (M_w = 900) the basic shape of the α transition remains unchanged. However with the addition of 25% HPL considerable changes are observed. The onset of the α transition has been shifted from 80°C for pure PMMA to 60°C for the 25% HPL/75% PMMA extruded blend. The transition is also noticeably broader. The addition of 40% HPL (M_w = 900) caused the onset temperature of the α-transition to be shifted to 30°C, some 50°C lower than that observed for pure PMMA. The shape of the α-transition is extremely broad and the development of a shoulder becomes apparent. This broadening of the α-transition and the onset of a shoulder is a clear indication of an immiscible system.

Figure 7B shows that an increase in HPL content causes blends containing an HPL of molecular weight 1390 (M_w) to exhibit α-transition changes similar to those found with an HPL of molecular weight 900 (M_w). With an addition of 25% HPL (M_w = 1390) no change in the α-transition is observed. However, with the addition of 25% HPL (M_w = 1390) a noticeable broadening of the α-transition is observed. For the 25% HPL/75% PMMA blend the onset of the α-transition is shifted from 80°C for pure PMMA to 60°C for the blend. The onset of the α-transition is shifted even further, to a temperature of 55°C, for the 40% HPL/60% PMMA blend. Along with the shift in α-transitions blends with HPL (M_w = 1390) levels of 25% and 40% developed a shoulder

on the low temperature side of the α-transition. This observance of a lowering of the onset temperature for the α-transition followed by the development of a shoulder on the α-transition is an indication of a two phase system. The initial lowering of the onset temperature for the α-transition could be an indication that at a 25% HPL level the PMMA is being plasticized. However the development of a shoulder at a 40% HPL level is a clear indication that a second T_g is being observed.

DMTA scans of blends made with a HPL that had a weight average molecular weight of 3300 are shown in Figure 6C. At a 5% HPL content a slight increase in the α-transitions onset temperature was once again observed and at 25% and 40% HPL contents a 20°C decreases in the α-transition's onset temperatures were observed. Some peak broadening was also observed at the 25% and 40% HPL contents. However, since the glass transition temperatures of the high molecular weight HPL and the PMMA are so close, 105°C and 110°C, respectively, results concerning the shapes of the curves are ambiguous.

Thus far no mention of the beta transition has been made, the reason being that it has remained relatively unchanged in all the blends. As noted earlier, this transition is the result of methyl ester side group rotations. Thus any environmental changes that occur with this side group should be observed in the beta transition. Very slight decreases in beta-transition magnitudes are noticed as HPL levels increase in all cases. However, this small decrease is believed to be the result of a decrease in the number of methyl ester

functional groups. It is believed that if secondary interactions occur between the benzene structure in lignin and the carbonyl group of PMMA, the rotation of the methyl ester group would be reduced resulting in a reduction of the loss modulus/storage modulus ratio (tan δ). However no such reduction is observed.

The objective of the first portion of the DMTA discussion was to describe the shape of the DMTA scans. Figures 7A, B and C show blends produced by injection molding. The solution cast blends showed scans with identical shapes with respect to broadening and the development of a shoulder, however actual onset temperatures and α-transition position did vary. A complete summary of the onset temperatures, T_g's (DMTA, DSC) and other thermal properties is found in Table 2.

As with the DSC data a single T_g (α-transition) was observed in all the DMTA scans. In order to more easily discuss the changes occurring with the T_g's (α-transitions) of the blends Figures 8A, B, C and D have been prepared. Once again for comparative purposes, T_g values predicted by the Flory-Fox equation are plotted along with the experimental data.

Figures 8A, B and C all show that the blend T_g values for the solution casted blends are relatively independent of HPL content, that is no change larger than 10°C is observed in any case, whereas the predicted T_g values change as much as 60° in the case where HPL of molecular weight 900 is blended with PMMA. The fact that the blend T_g is independent of HPL content indicates that an immiscible, phase-separated system is present and no interactions between blend

components are occurring. Therefore it is believed that the α-transitions of blends containing HPL (unfr., M_w = 900 and M_w = 1390) are that of uninhibited PMMA. Slight changes in the α-transitions can be attributed to the overlapping of a second T_g, that of HPL, which is seen as a low temperature shoulder observed earlier in Figures 7A, B and C.

As was observed with the DSC data Figures 8A, B and C show that the injection molded samples follow the same trend of decreasing T_g value with increasing HPL content seen with the predicted T_g data. Once again indicating that blends prepared by injection molding are more homogeneous than those prepared by solution casting. However in Figure 8D, which shows data for blends of PMMA and HPL of mol. wt. 3300, the predicted T_g data shows a slight decrease in T_g with increasing HPL content. Whereas the injection molded blends show an increase in T_g, above that of the parent polymers, with increasing HPL content. This same increase in T_g above that of the parent polymers is also observed at the 5% HPL level of injection molded blends seen in Figures 8A, B and C. An increase in T_g above that of the parent polymers is rare in polyblends but has been reported with other blended systems (25). This phenomenon has been explained by the presence of very strong polymer-polymer interactions that act as quasi crosslinks therefore resisting molecular motion which results in an increase in T_g. Deviations from linear models (Flory-Fox) as seen with the injection molded data of Figures 8A, B and C have also been attributed to the presence of polymer-polymer interactions (26).

Another explanation for the presence of T_g's above that of the parent polymers is that in the process of injection molding the blend polymers are "locked" into non-equilibrium conformations that have less free volume and thus higher T_g's.

Mechanical Properties

When two polymers are blended and form a homogeneous single-phase system the modulus of elasticity for that system is roughly intermediate that of the two parent polymers. On the other hand, when two polymers exist in separate phases the relationship between composition and modulus is not nearly as simple. In one view, the structure which is present in the largest amount should form the continuous matrix phase and play the primary role in determining mechanical properties. The role of the secondary phase will be dictated by the interphase between the domains and the matrix. In other words, the degree of miscibility and the extent of interfacial adhesion govern the ultimate mechanical performance of a blend in the solid state.

SEM and thermal analysis of HPL/PMMA blends have indicated that these blends form phase separated systems. However, differences have been observed by SEM between solution cast and injection molded blends in terms of their domain-matrix interphase. Solution cast blends formed domains that were pulled away from the matrix indicating little or no association at the interphase. This type of interphase would suggest that the HPL domains are acting as a filler and are not

actively involved in the mechanical properties of the blends. On the other hand blends prepared by injection molding did not show visible domain-matrix separation therefore better association at the interphase is assumed. Association at the domain-matrix interphase would suggest that the HPL domains are more actively involved in the mechanical properties of the injection molded blends.

Figure 9A shows the change in Young's modulus with HPL content for blends containing unfractionated HPL and PMMA. Also included in Figures 9A-D is the predicted Young's modulus which was calculated using equation 5 (27):

$$E_c = E_1 V_1 + E_2 V_2 \qquad \text{(Eq. 5)}$$

where E_c = moduli of composite

$E_{1,2}$ = moduli of composite 1,2

$V_{1,2}$ = volume fraction composite 1,2

Equation 5 is typically used to predict the modulus of polymer composites or filled systems. It is used in Figure 9 for comparative purposes. In Figures 9A-D the injection molded blend containing 5% HPL showed a much larger increase in modulus than predicted by the model. Whereas both solution cast blends show lower than predicted modulus values. At 25% and 40% HPL levels the injection molded blends and blends cast with chloroform showed increases in modulus; however blends cast with THF showed decreases in modulus at these same HPL levels. Figures 9B, C and D, which show Young's modulus data for blends containing HPL of molecular weight (M_w) 990, 1390 and 3300, respectively, indicate that at 5% HPL content injection molded and chloroform cast blends show higher than predicted modulus values.

However only the injection molded blends show continued increases in modulus at 25% and 40% HPL contents as predicted by equation 5.

The fact that the modulus data for injection molded and chloroform cast blends containing 5% HPL were consistently higher than those of the predicted modulus indicates that the high modulus HPL (2000 MPa) (28) is "more actively involved" in the material's modulus than suggested by a simple weighted average model. However when comparing data from Figures 9A, B, C and D blends prepared by injection molding are the only blends that consistently show the predicted increase in modulus with an increase in HPL content. Therefore the modulus data for blends prepared by injection molding indicates that HPL (unfr. M_w = 900, 1390 or 3300) influences the Young's modulus thus indicating some degree of interaction between PMMA and HPL. The degree of "interaction" or "association" is unclear since the T_g data from DMTA and DSC only suggested the possibility of polymer-polymer interaction. Also analysis of DMTA beta transitions did not indicate the presence of polymer-polymer interaction in the injection molded blends.

It should also be pointed out that for the injection molded blends the modulus at a given HPL content never changed more than 10 Mpa with a change in HPL molecular weight. In other words at a given HPL content the moduli were fairly constant and showed no significant dependence on HPL molecular weight. The solution cast modulus data were inconsistent in terms of HPL molecular weight and is believed to be dictated by the presence of the large domains seen by SEM. These domains act as crack propagation sites and also reduce the true cross-sectional area of the blend. Hence no clear relationship

between modulus and HPL molecular weight for solution cast blends was seen.

Since lignin is a high modulus glassy material it would not be considered a tensile builder. This assumption is made apparent in Figures 10A, B and C. It is clear that solution cast and extruded samples all showed noticeable decreases in tensile strength with increased HPL content. However neither solution casting or injection molding showed any consistent tensile strength-HPL molecular weight dependencies. Therefore under the given molecular weight range, tensile strength of HPL/PMMA blends was found to be independent of HPL molecular weight. Figures 10A, B and C also indicate, especially at 5% and 25% HPL levels, that the injection molded blends have higher tensile strength values than those of the solution cast blends. This is possibly an indication of polymer-polymer association suggested earlier by SEM, DSC and DMTA. However at high concentrations of HPL blends casted from chloroform show tensile strength values comparable to those of injection molded blends.

Figures 11A, B and C show that the ultimate strain of all HPL/PMMA blends is reduced with increased HPL content. Furthermore, ultimate strain is also found to be independent of HPL molecular weight. Once again blends prepared by injection molding show significantly higher values than those found for the solution cast blends, especially at 5% and 25% HPL contents. Thus indicating the possibility of polymer-polymer association or interaction in the injection molded blends.

Conclusions

1) Blends of PMMA and various molecular weight HPL's formed two phase systems. SEM results show that solution cast blends form distinct domains whereas injection molding creates a blend in which the HPL is found in striations of various widths. This two phase system is also indicated by DSC where a first scan shows two endotherms. These are believed to be the result of enthalpy relaxation in the respective polymer. A second scan shows a single broad T_g which is believed to be the result of an overlapping of the two T_g's or transitional smearing. Another indication of a two phase system was seen with DMTA where a shoulder, which coincides with the T_g of HPL, developed with increasing HPL content.

2) The interphase between the domains and matrix of the blends differed with respect to the method of preparation. Solution cast blends showed domains that were "pulled away" from the matrix whereas the injection molded blends showed HPL striations that were closely associated with the matrix. The fast time of vitrification experienced by the injection molded samples "locked" the polymers in a randomly mixed state whereas the slower time of vitrification for the solution casted blends allowed domains of large dimensions to form (1 μm to 14 μm).

3) The close proximity of the domains and matrix observed by SEM in injection molded samples indicated the possibility of polymer-polymer interactions. Interactions were also suggested by the T_g data from DSC and DMTA. Both DSC and DMTA T_g values followed the same trends shown by the Flory-Fox equation, thus indicating some

degree of miscibility. However, the injection molded blend T_g values were consistently higher in magnitude than those predicted. Such deviations from linear models (Flory-Fox) have been described as the result of polymer-polymer interactions. Whether or not the trends and deviations observed with the HPL/PMMA blend T_g's are an indication of miscibility and interactions is unclear since the single T_g's shown by the blends are believed to be the result of transitional smearing.

4) Analysis of DMTA beta transitions indicated that polymer-polymer interactions involving the carbonyl group of PMMA did not occur. The beta transition in PMMA is reportedly due to the movement of the methyl ester side group of PMMA. A change in the environment of the methyl ester group would result in a change in the temperature and shape of the transition, no such changes were observed with the injection molded or solution cast blends. Previous studies have shown interactions between carbonyl groups and aromatic structures; however, such interactions were not observed by the methods of analysis used in this study.

5) The addition of HPL to PMMA was found to cause an increase in modulus. With the addition of 5% HPL a very large initial increase in modulus was observed. Whereas the addition of 25% and 40% HPL showed relatively small increases when compared to that observed with the 5% HPL. The addition of 25% and 40% HPL in injection molded blends resulted in modulus changes that closely followed a rule of mixture based model. Blends cast from solution did not show consistent data. This is again attributed to the large domains which would act as crack propagation sites and reduce the true cross sectional area. The fact

that the injection molded blends showed the expected increase in modulus with an increase in HPL content indicates that the HPL is actively involved in the material properties thus suggesting some degree of polymer-polymer association is occurring.

6) The addition of HPL to PMMA caused a decrease in ultimate properties, tensile strength and ultimate strain. Such decreases were expected since lignin is a high modulus glassy material with a relatively low molecular weight, when compared to commercially used polymers. Once again the injection molded blends showed consistently higher values than the solution cast blends. This is especially apparent at 5% HPL. Possible association in the injection molded blends would allow the 5% HPL blends to maintain their ultimate properties.

7) The range of HPL molecular weights used in this study had no significant effect on the material properties of the HPL/PMMA blends. In relation to typical commercial polymers the range of molecular weights (reported as M_w from 900 to 3300) was very narrow thus no large changes in properties were expected. However, domains in the solution cast blends were found to increase in size with increasing molecular weight.

Literature Cited

1) "Polymer Blends", Polym. Eng. Sci., 22(2) (1982).

2) D. R. Paul and J. W. Barlow, J. Macromol. Sci.-Rev. Macromol. Chem., C18, 109 (1980).

3) A. Pavan, T. Ricco and M. Rink, Mater. Sci. Eng., 45, 201 (1980).

4) A. Pavan, T. Ricco and M. Rink, Mater. Sci. Eng., 48, 9 (1981).

5) G. D. Cooper et al., Materials Technology, p. 21 (1981).

6) S. T. Wellinghoft, J. L. Koenig and E. Baer, J. Polym. Sci., Polym. Phys. Ed., 15, 1913 (1977).

7) A. Rudin, "The Elements of Polymer Science and Engineering", Academic Press, New York, N.Y. 1982, Chapter 12.

8) G. Scatchard, Chem. REv. 8, 321 (1931).

9) J. H. Hildebrand, J. M. Pravsnitz, and R. L. Scott, "Regular and Related Solutions". Van Nostrand Reinhold, New York, 1970.

10) L. C.-F. Wu and W. G. Glasser, J. Appl. Polym. Sci., 29, 1111 (1984).

11) E. E. Underwood, "Quantitative Stereology", Addison-Wesley Pub. Co., Reading, Massachusetts (1970).

12) W. G. Glasser, C. A. Barnett, T. G. Rials, and V. P. Saraf, J. Appl. Polym. Sci., 29, 1815-1830 (1984).

13) S. Sarkanen, D. C. Teller, J. Hall, and J. L. McCarthy, Macromol., 14, 426 (1981).

14) W. Lange, O. Faix, and O. Beinhoff, Holzforsch., 37, 63 (1983).

15) Kelley, S. S., Ph.D. Dissertation, VPI & SU, 1986.

16) P. J. Corish and M. J. Palmer, "Advances in Polymer Blends and Reinforcements", Inst. Rubber Ind. Conf., Loughborough (1969).

17) T. G. Fox, Bull. Am. Phys. Soc., 1, 123 (1956).

18) F. W. Billmeyer, "Textbook of Polymer Science", Wiley: New York (1984).

19) Z. G. Gardlund, "Properties and Morphology of Poly(methyl Methacrylate/Bisphenol A Polycarbonate Blends", Adv. Chem. Ser. No. 206 (1984).

20) E. A. Turi, et al., "Thermal Characterization of Polymer Materials", Academic Press, New York, N.Y., p. 881 (1981).

21) W. J. MacKnight, R. E. Karasz, and J. R. Fried, in "Polymer Blends Vol. 1 and 2", (D. R. Paul and S. Newman, Eds.), Academic Press, New York, p. 224-228 (1978).

22) T. G. Rials, J. Wood Chem. and Techn., 4(3), p. 331-345 (1984).

23) T. K. Kwei, J. Appl. Polym. Sci., 22, p. 307-313 (1984).

24) N. G. McCrum, B. E. Read, G. Williams, "Anelastic and Dielectric Effects ini Polymer Solids", Wiley, New York, N.Y. (1967).

25) J. R. Pennacchia, E. M. Pearce, T. K. Kwei, B. J. Bulkin, and J. P. Chen, Macromolecules (20), pp. 50-55 (1985).

26) M. Gordon and J. S. Taylor, J. Appl. Chem., 2, 493 (1952).

27) R. P. Sheldon, "Composite Polymeric Materials", Applied Science Publishers, New York, N.Y. (1982).

28) S. I. Falkehag, Appl. Polym. Symp. 28, p. 247 (1975).

List of Tables and Figures

Figure 10. The variation in tensile strength with the addition of unfractionated HPL, HPL M_w = 900 "low", HPL M_w = 1390 "medium", and HPL M_w = 3300 "high" where A) blends prepared by injection molding, B) blends prepared by solution casting with chloroform, C) blends prepared by solution casting with THF.

Figure 11. The variation in ultimate strain with the addition of unfractionated HPL, HPL M_w = 900 "low, HPL M_w = 1390 "medium", HPL M_w = 3300 "high" where A) blends prepared by injection molding, B) blends prepared by solution casting with THF, C) blends prepared by solution casting with chloroform.

TABLE 1. SUMMARY OF HPL Fractions Isolation, Glass Transition and Molecular Weight Data

Fraction #	Acetone/Hexane ratio	Percent of material	Tg°C	Mol. wt. GPC (THF)	Mol. wt (THF) GPC/Viscosity	(*) Mol. wt. GPC (DMF)	Mol. wt. VPO (DMF)
1 ("Low")	.8	40%	30°C	$\bar{M}_n$ = 520 $\bar{M}_w$ = 900	$\bar{M}_n$ = 950 $\bar{M}_w$ = 4,430	$\bar{M}_n$ = 1,900 $\bar{M}_w$ = 2,300	$\bar{M}_n$ = 1,700
2 ("Medium")	1	16%	68°C	$\bar{M}_n$ = 730 $\bar{M}_w$ = 1,390	$\bar{M}_n$ = 1,300 $\bar{M}_w$ = 4,200	$\bar{M}_n$ = 2,300 $\bar{M}_w$ = 4,800	$\bar{M}_n$ = 2,100
3	2	9%	87°C	$\bar{M}_n$ = 730 $\bar{M}_w$ = 1,550	$\bar{M}_n$ = 5,500 $\bar{M}_w$ = 10,280	$\bar{M}_n$ = 3,260 $\bar{M}_w$ = 5,900	$\bar{M}_n$ = 2,800
4 ("Medium")	ppt.	20%	105°C	$\bar{M}_n$ = 1,300 $\bar{M}_w$ = 3,300	$\bar{M}_n$ = 1,900 $\bar{M}_w$ = 63,000	$\bar{M}_n$ = 10,000 $\bar{M}_w$ = 33,000	

$\sum$ = 85%

(*) Data from Kelley, S.S., Ph.D. Dissertation, VPI&SU, 1986.

TABLE 2. Summary of HPL/PMMA Blend Thermal Analysis Data

Sample	%HPL	# of Trans. 1st scan DSC	Tg °C DSC	Tg °C DMTA	Breadth of Tg DSC	Breadth of Tg DMTA	Onset of α- trans.	Shoulder on α- trans.
CHOLORFORM								
PURE PMMA		1	87.5	104	43	15	68	no
UNFRACTIONATED	5%	1	87	107	45	34	60	no
(HPL)	25%	2	90	106	45	37	60	no
	40%	2	74	106	63	37	54	yes
HPL (M_w = 900)	5%	1	84.5	100	30	30	60	no
	25%	2	82	100	49	30	30	yes
	40%	2	80	96	75	32	32	yes
HPL (M_w = 1390)	5%	1	74	99	58	33	55	no
	25%	2	87.5	99	50	34	45	no
	40%	2	80	105	70	31	50	yes
HPL (M_w = 3300)	5%	1	80.7	94	30	39	55	no
	25%	1	85	98	38	34	63	no
	40%	1	84	110	27	36	60	no
THF								
PURE PMMA		1	93	108	36	22	68	no
UNFRACTIONATED	5%	1	94	103	38	28	70	no
	25%	2	91	101	48	25	73	no
	40%	2	89	99	62	24	72	yes
HPL (M_w = 900)	5%	1	88	115	50	27	75	no
	25%	2	91	110	51	25	52	yes
	40%	2	86	102	50	22	55	yes
HPL (M_w = 1390)	5%	2	97	110	53	34	70	no
	25%	2	95	110	61	28	55	yes
	40%	2	87	104	59	27	50	yes
HPL (M_w = 3300)	5%	1	98	107	27	29	66	no
	25%	2	110	118	28	30	75	no
	40%	2	108	116	26	25	70	no
EXTRUDED								
PURE PMMA		1	109	112	27	24	77	no
UNFRACTIONATED	5%	1	112	118	36	22	70	no
	25%	2	99	111	55	27	65	no
	40%	2	98	105	57	32	50	yes
HPL (M_w = 900)	5%	1	102	119	82	22	75	no
	25%	2	91	99	53	28	52	yes
	40%	2	70	90	60	36	29	yes
HPL (M_w = 1390)	5%	1	108	113	46	23	75	no
	25%	2	93	102	55	33	55	yes
	40%	2	90	99	52	31	46	yes
HPL (M_w = 3300)	5%	1	112	118	36	21	85	no
	25%	2	103	118	60	27	70	no
	40%	2	116	122	33	27	70	no

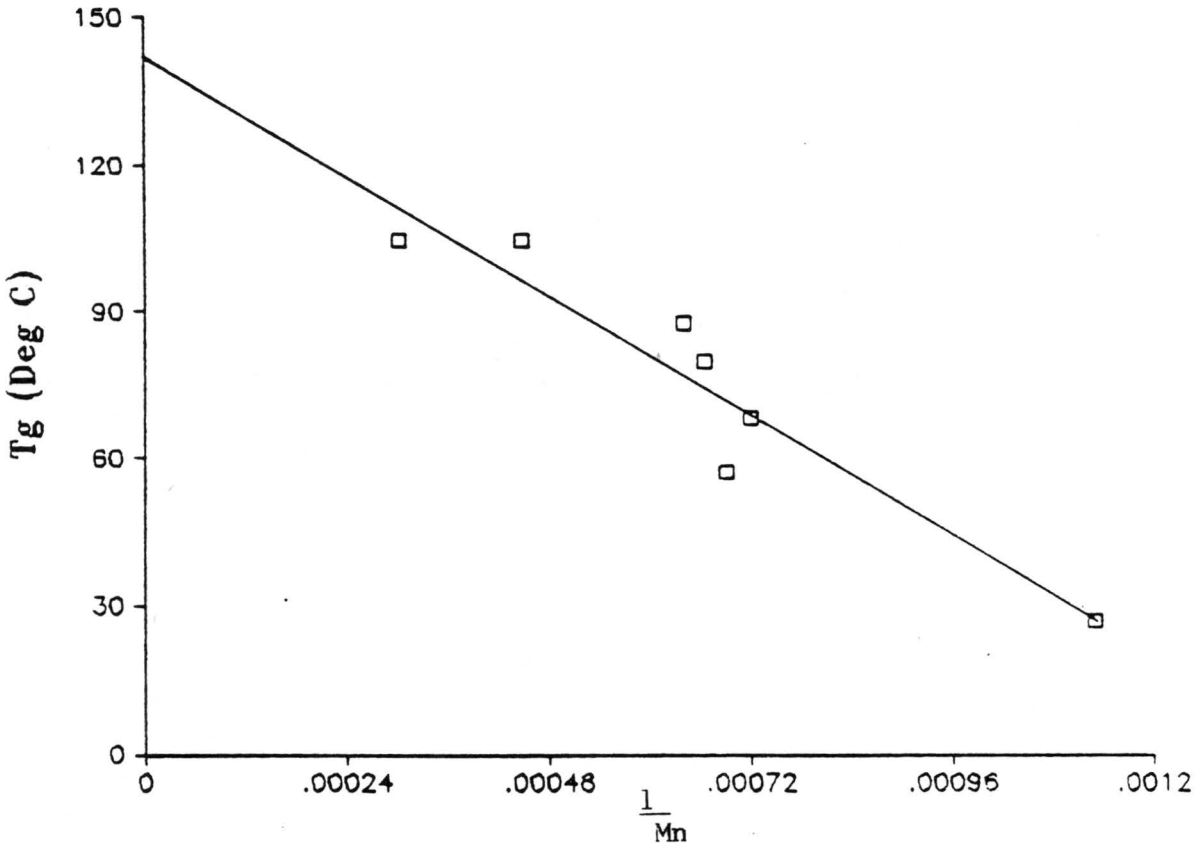

Figure 1. The relationship between T_g and $1/M_n$.

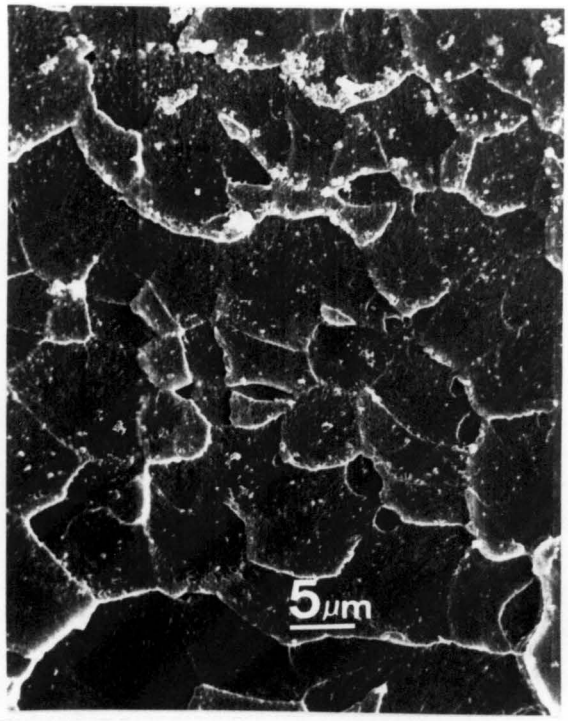

Figure 2 (A) Pure PMMA 1000 X

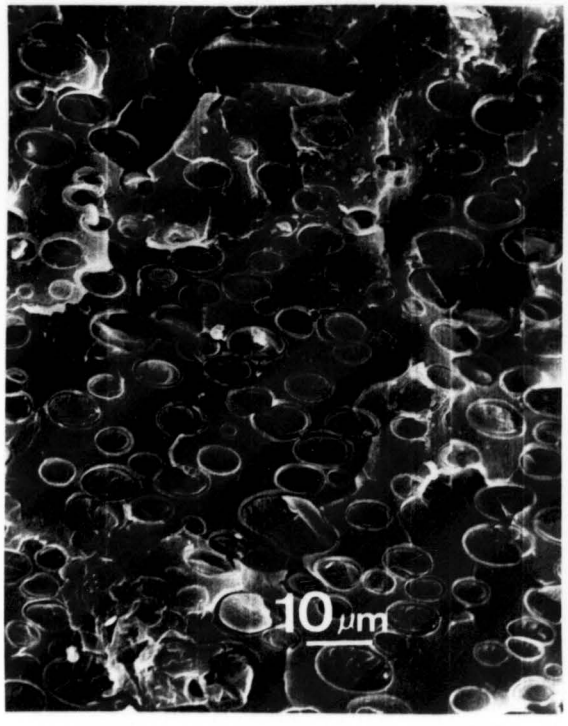

Figure 2 (B) 25% HPL / 75% PMMA Solution Cast with (THF) 1000 X

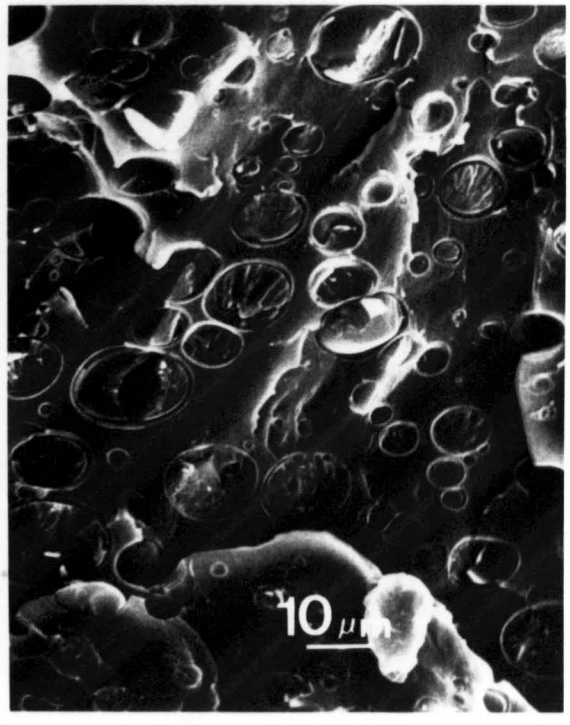

Figure 2 (C) 25% HPL / 75% PMMA Solution Cast with (Chloroform) 1000 X

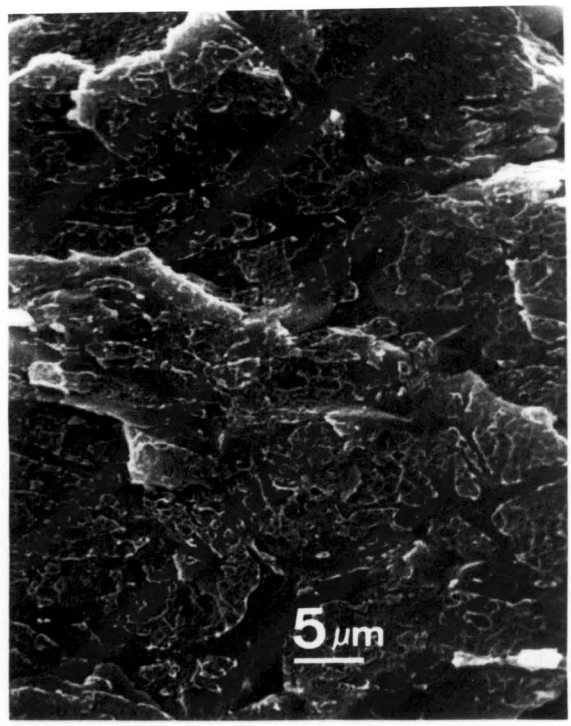

Figure 2 (D) 25% HPL / 75% PMMA (Injection Molded)
2000 X

Figure 2 (E) 25% HPL / 75% PMMA (Injection Molded)
5000 X Etched

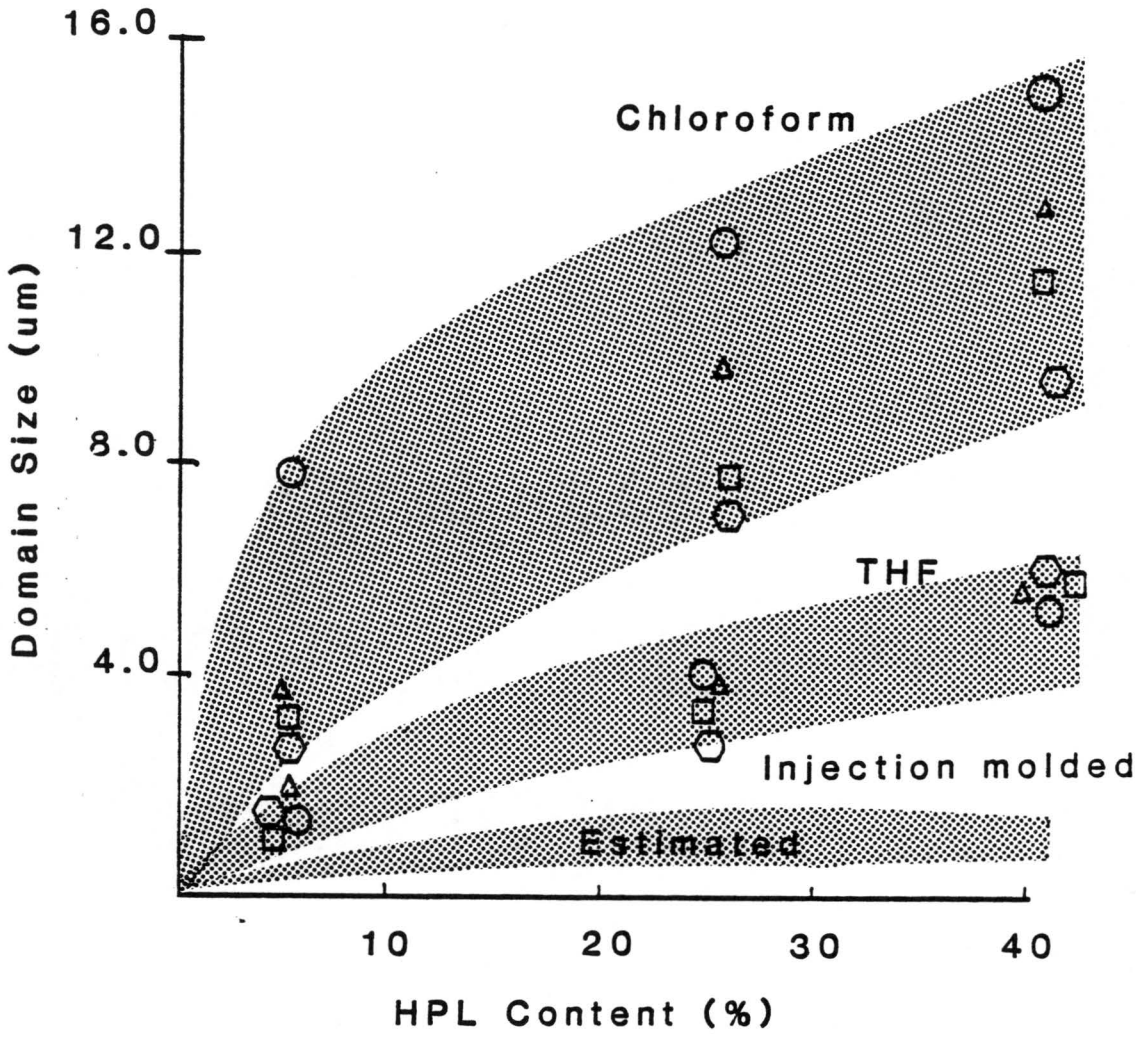

Figure 3. The relationship between domain size (um) and HPL content where (□) unfractionated HPL (⬡) HPL of M_w = 900 "Low" (△) HPL of M_w = 1390 "medium" (○) HPL of M_w 3300 "high".

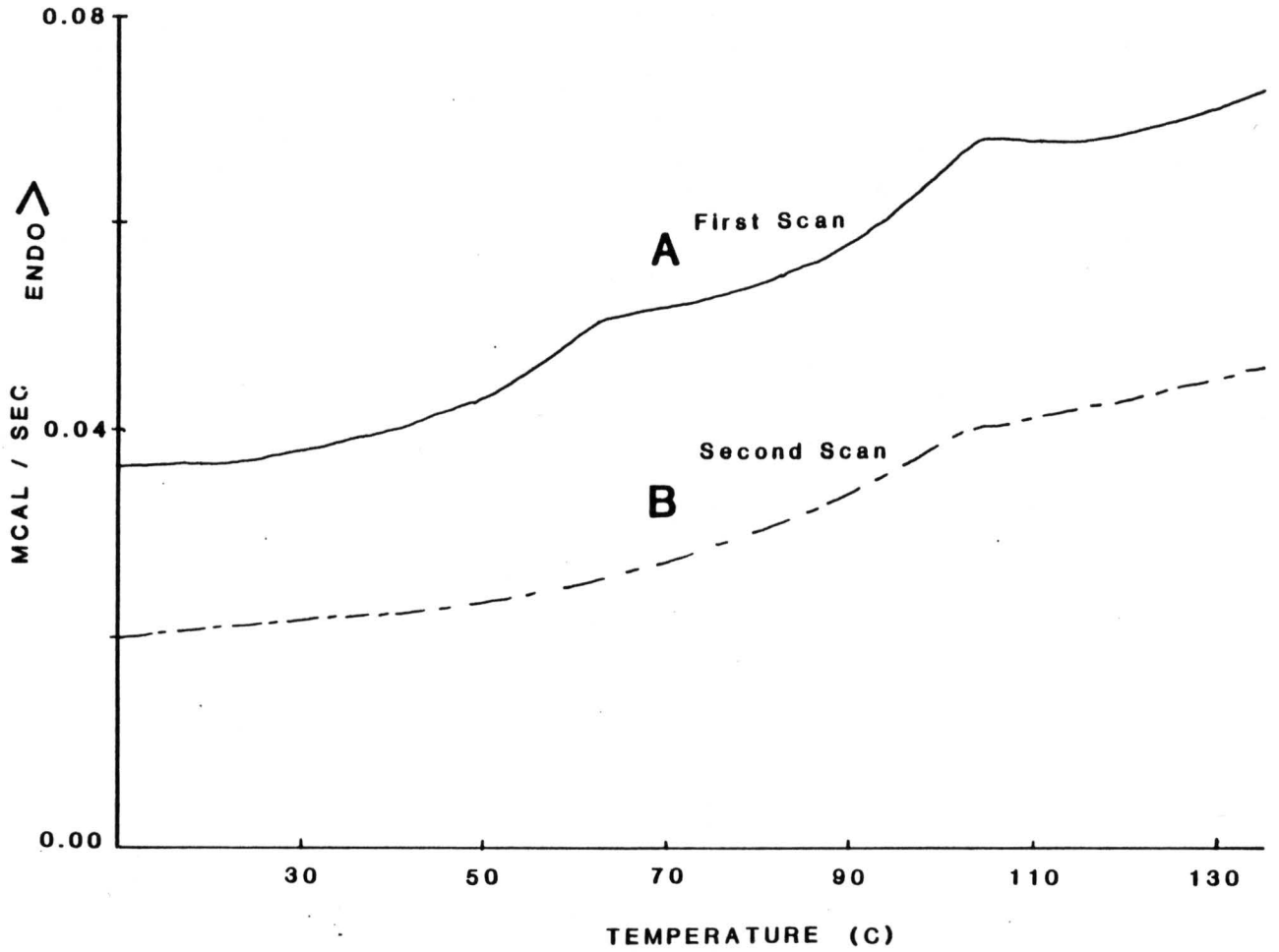

Figure 4. Typical DSC trace of HPL/PMMA blends. A) initial scan, B) rescanned immediately after cooling.

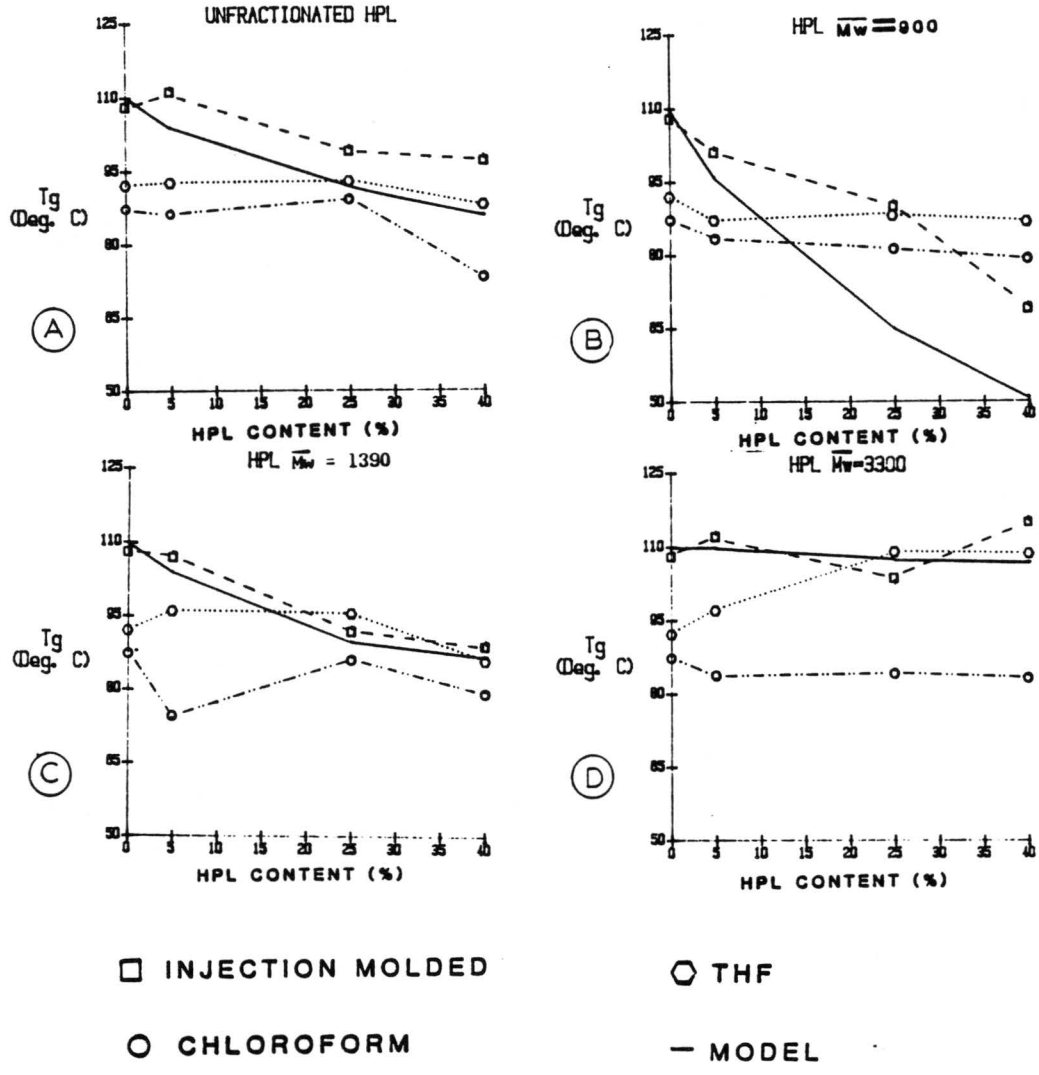

Figure 5. The relationship between HPL/PMMA blend T_g and HPL content as determined by DSC where A) unfractionated HPL, B) HPL M_w = 900 "low", C) HPL M_w = 1390 "medium", D) HPL M_w = 3300 "High".

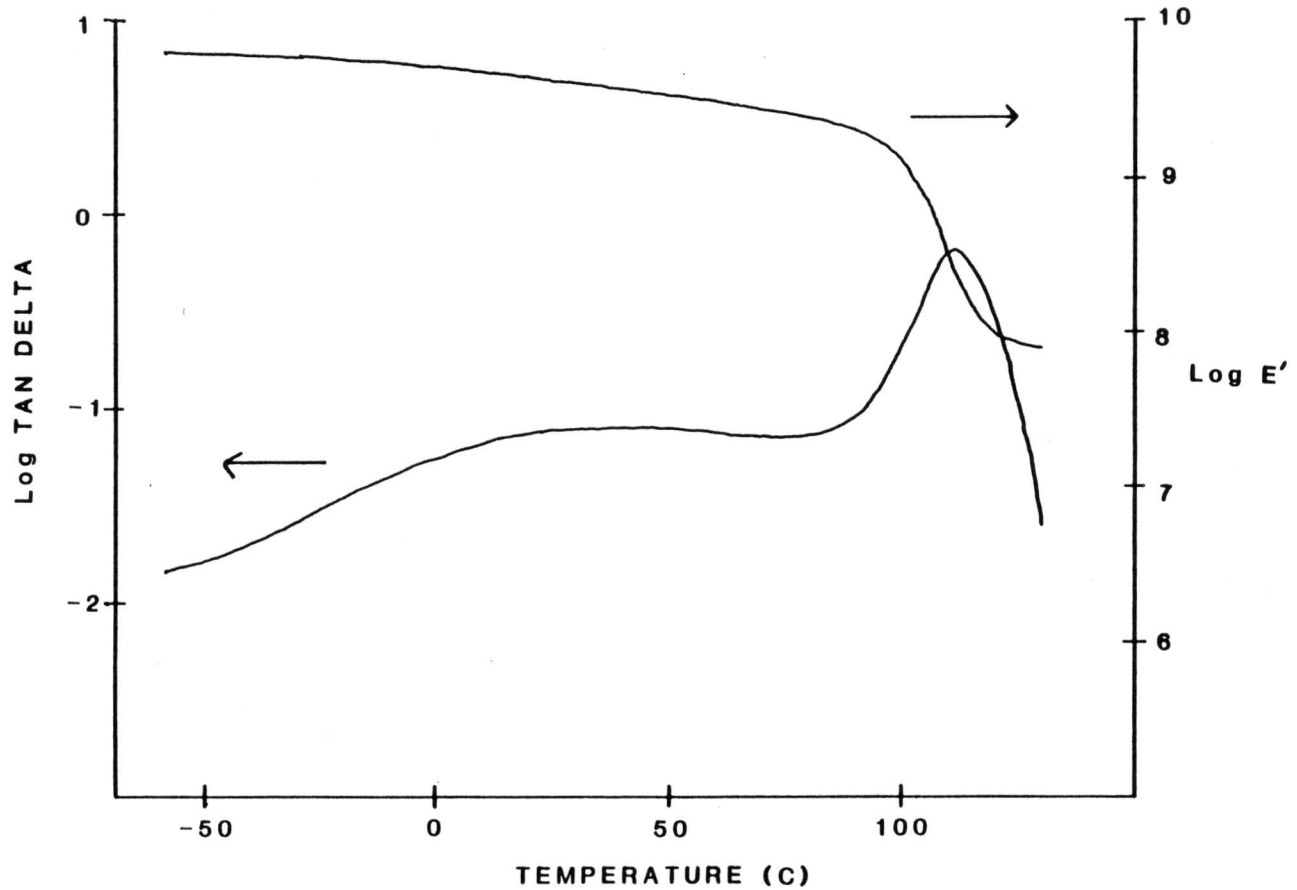

Figure 6. The variation in log $\tan \delta$ with temperature for PMMA

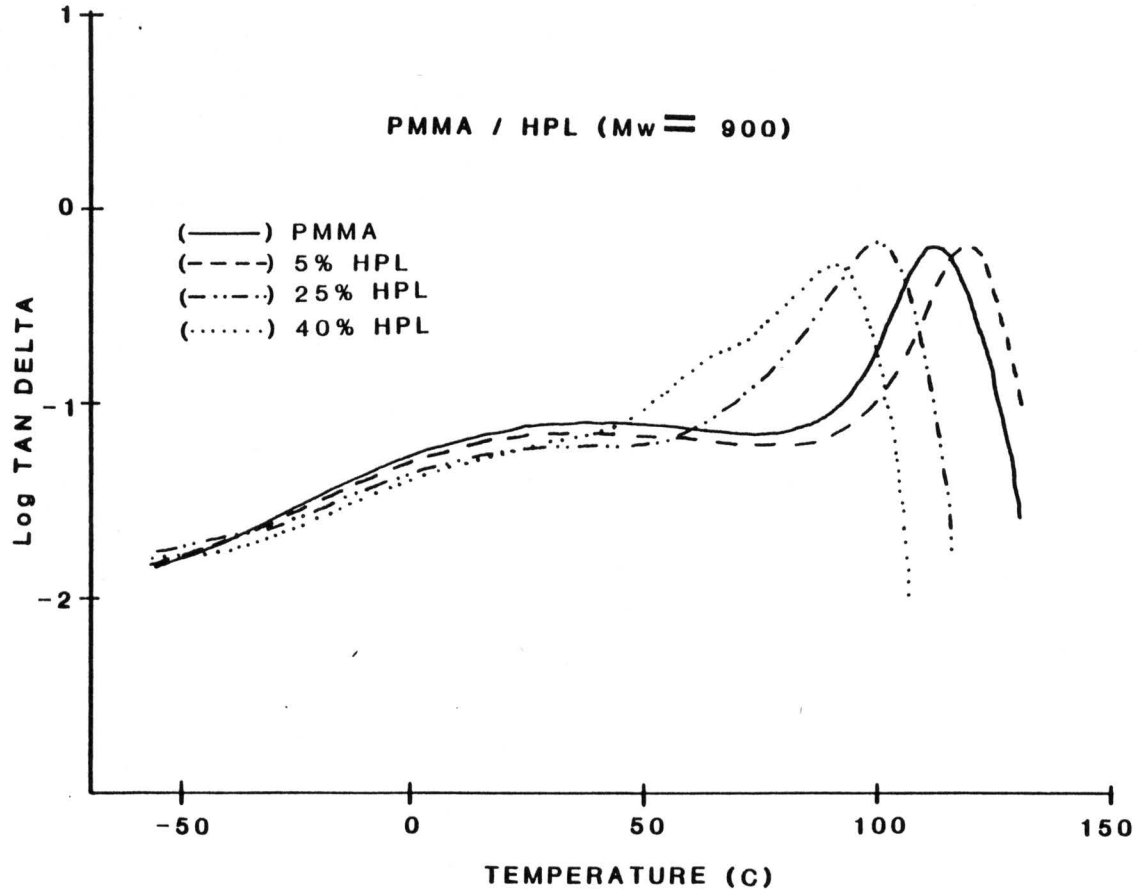

Figure 7A. The variation in log tan δ with temperature for blend of HPL M_w = 900 "low"/PMMA where (——) PMMA, (– –) 5% HPL (–··) 25% HPL (····) 40% HPL.

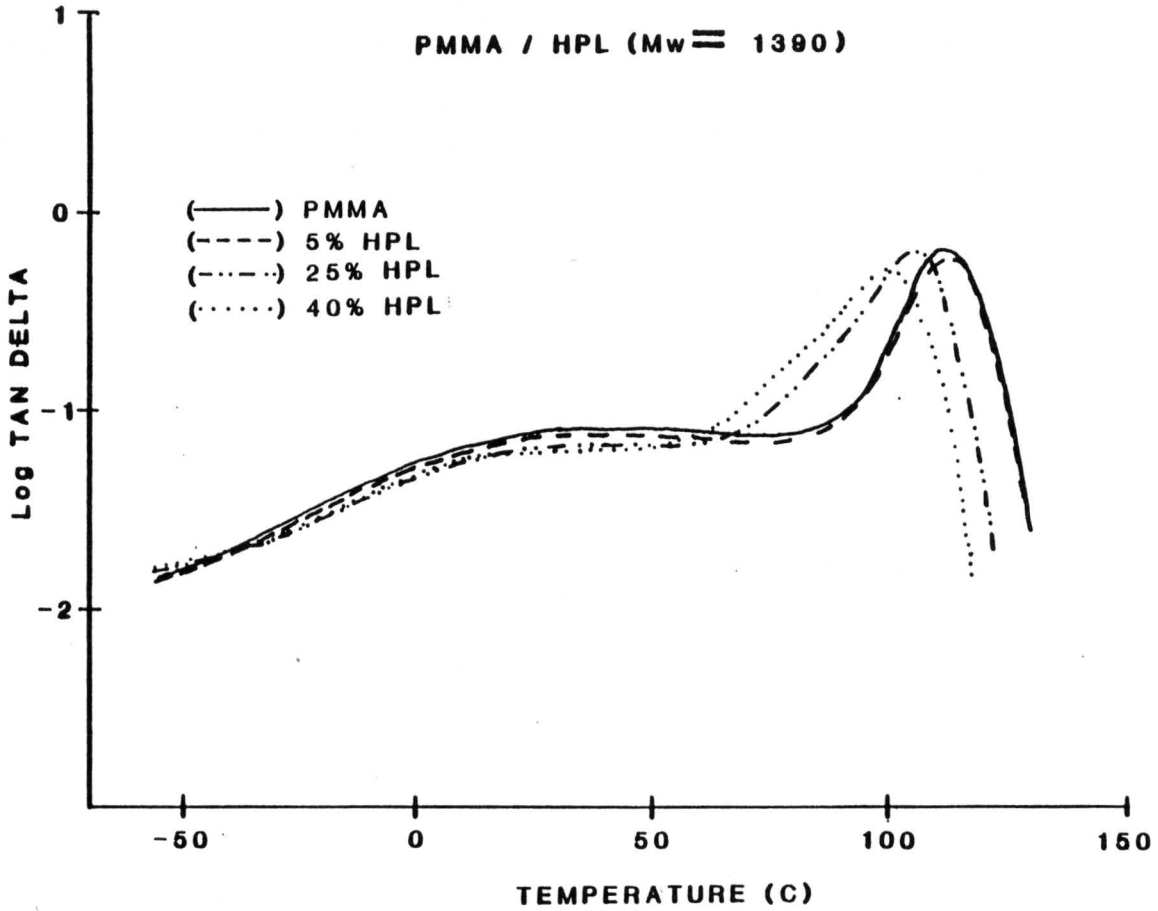

Figure 7B. The variation in log tan δ with temperature for blend of HPL Mw = 1390 "medium"/PMMA where (——) PMMA, (- -) 5% HPL(-·) 25% HPL (·····) 40% HPL.

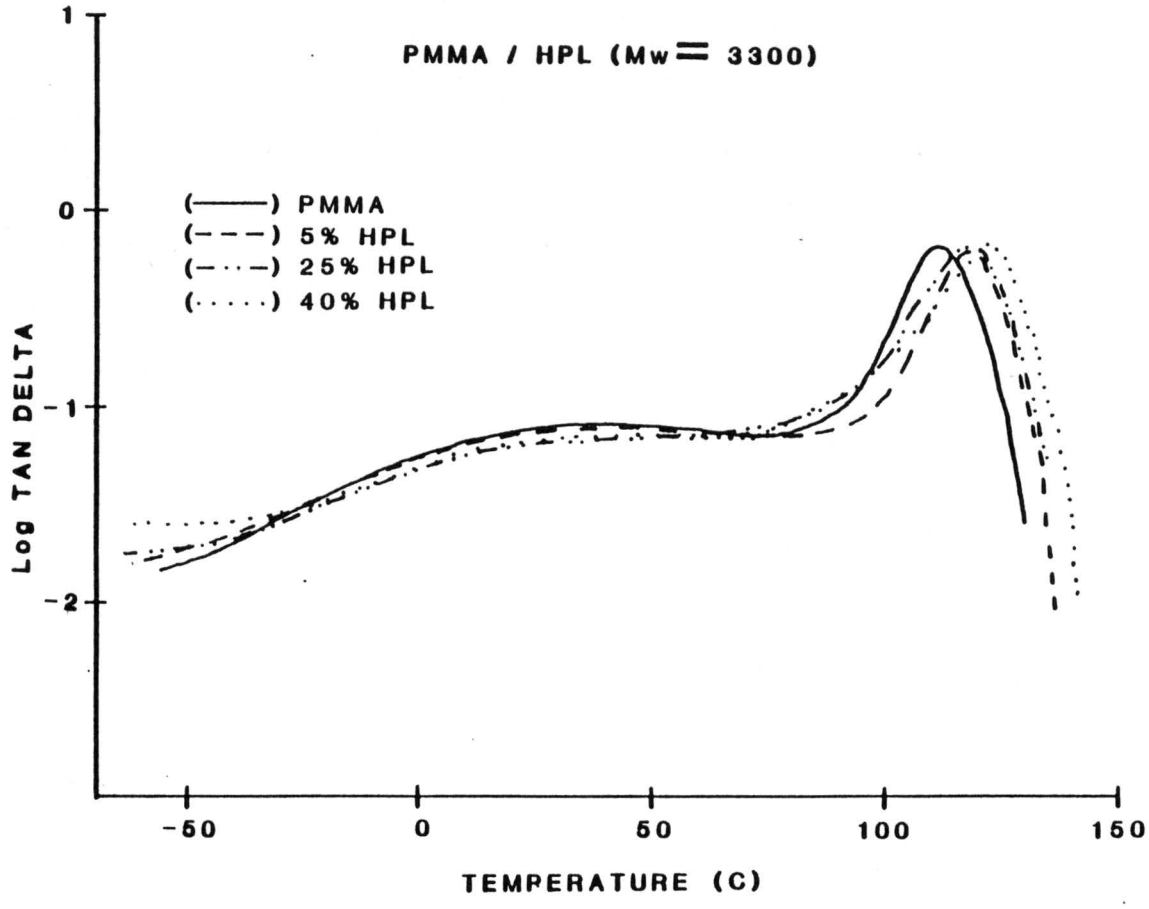

Figure 7C. The variation in log tan δ with temperature for blend of HPL M_w = 3300 "high"/PMMA where (——) PMMA, (– –) 5% HPL (–··) 25% HPL (···) 40% HPL.

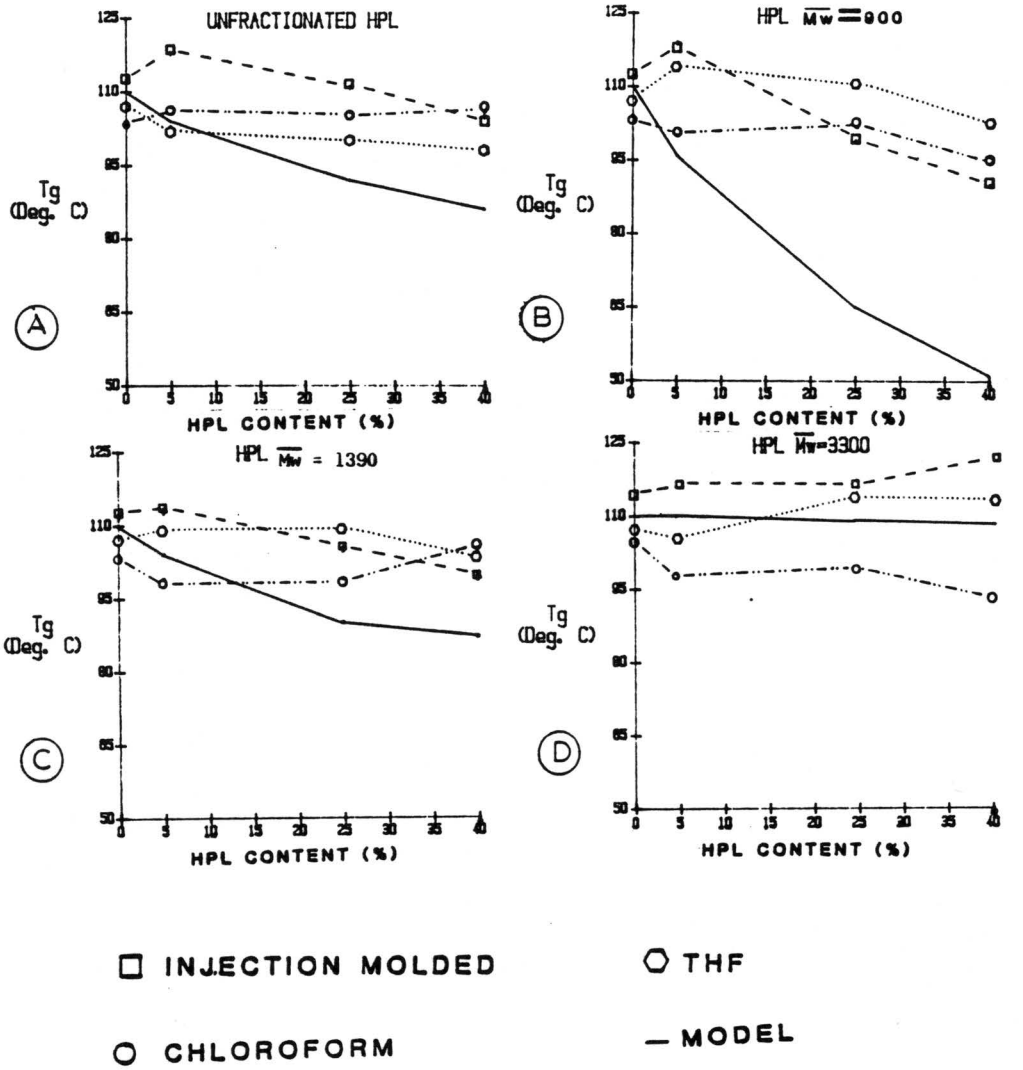

Figure 8. The relationship between HPL/PMMA blend T_g and HPL content as determined by DMTA where A) unfractionated HPL, B) HPL M_w = 900 "low", C) HPL M_w = 1390 "medium", D) HPL M_w = 3300 "high".

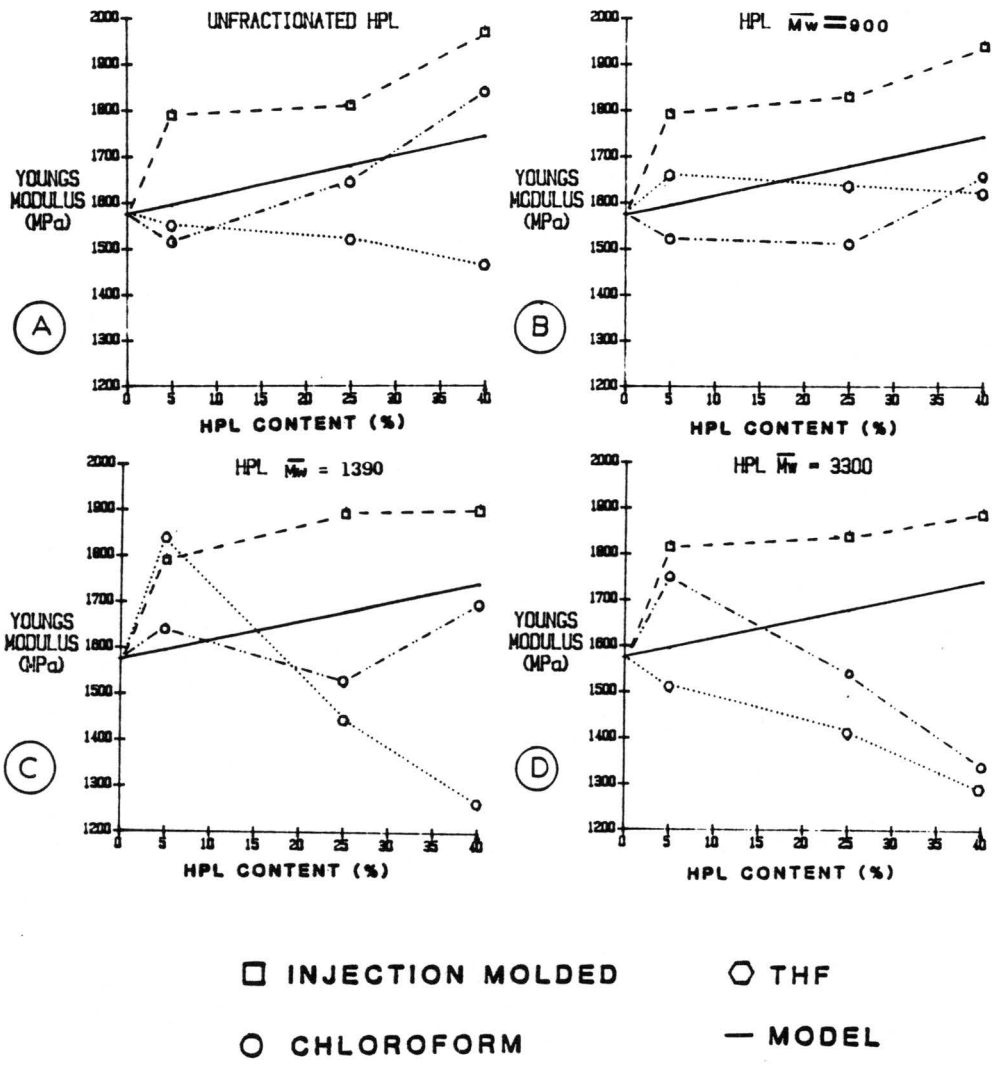

Figure 9. The variation in blend Young's modulus with HPL content where A) unfractionated HPL, B) HPL M_w = 900 "low", C) HPL M_w = 1390 "med m", D) HPL M_w = 3300 "high".

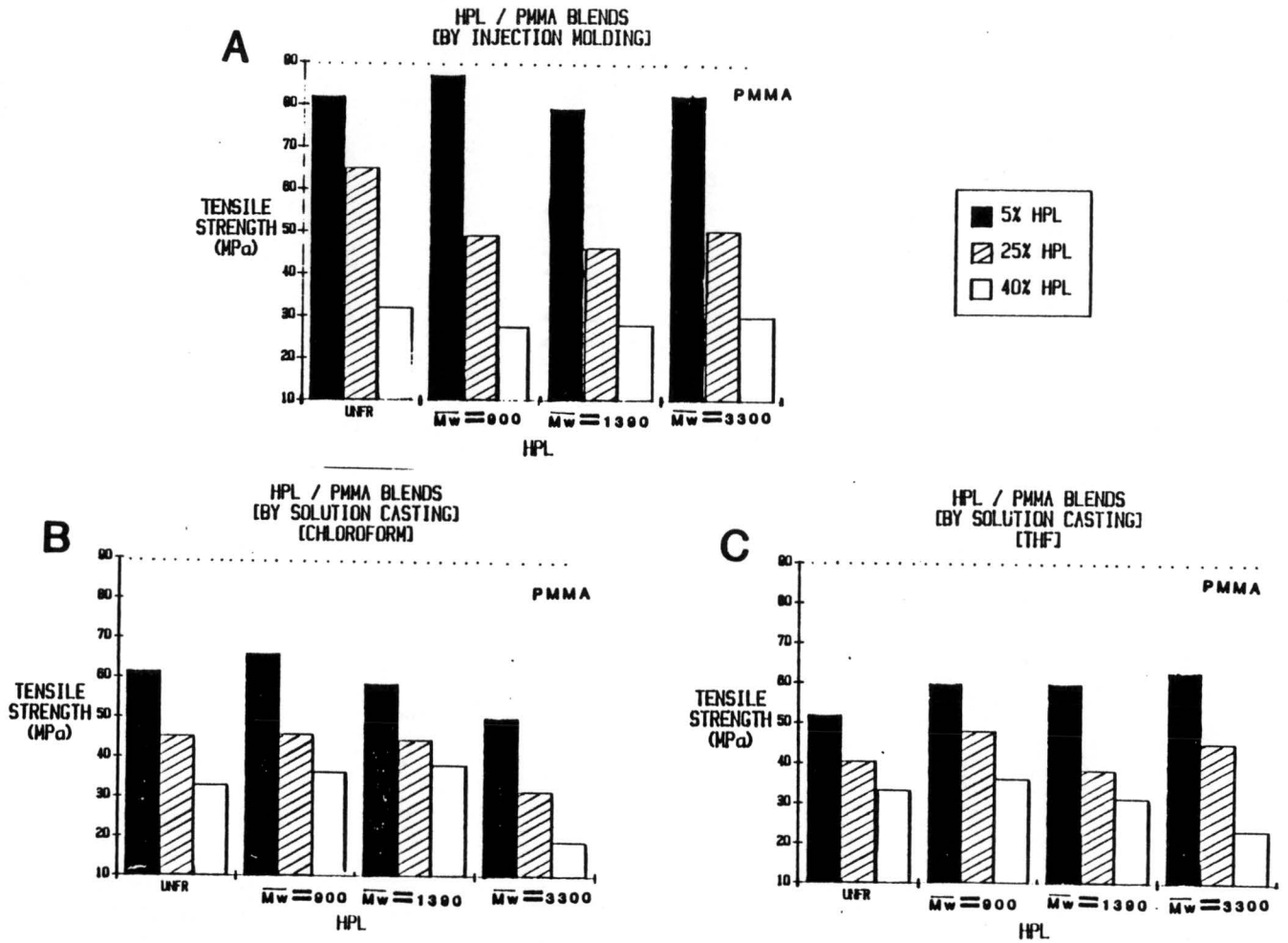

Fig. 10. The variation in tensile strength with the addition of unfractionated HPL, HPL M_w = 900 "low", HPL M_w = 1390 "medium", and HPL M_w = 3300 "high" where A) prepared by injection molding, B) prepared with chloroform, C) prepared with THF.

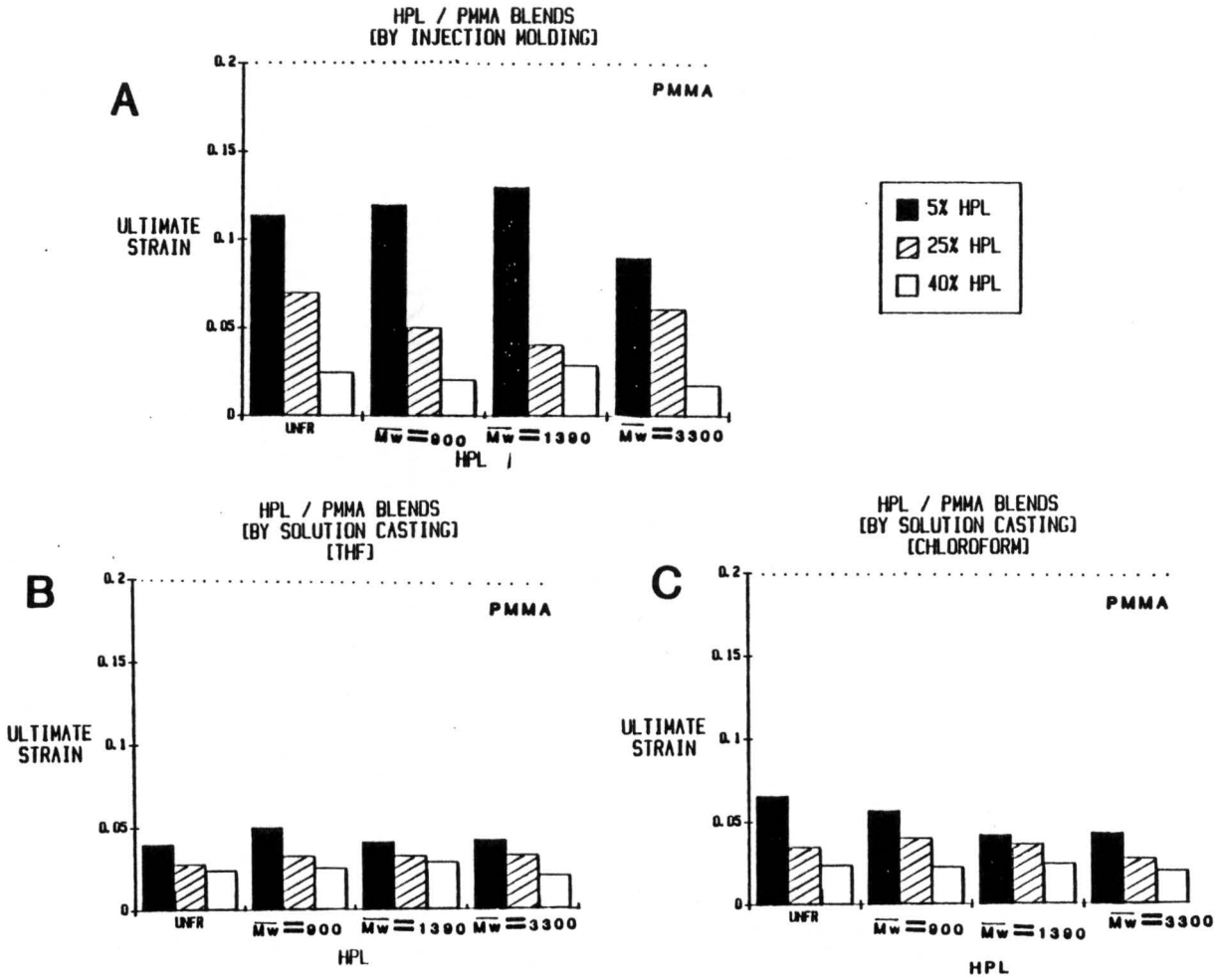

Fig. 11. The variation in ultimate strain strength with the addition of unfractionated HPL, HPL M_w = 900 "low", HPL M_w = 1390 "medium", and HPL M_w = 3300 "high" where A) prepared by injection molding, B) prepared with chloroform, C) prepared with THF.

CHAPTER 2: A STUDY OF THE MISCIBILITY AND POLYMER-POLYMER INTERACTIONS IN HYDROXYPROPYL LIGNIN/POLY(VINYL ALCOHOL) BLENDS

(ABSTRACT)

Polymer blends consisting of hydroxypropyl lignin and poly(vinyl alcohol) were prepared by solution casting and evaluated in terms of HPL content and poly(vinyl alcohol)'s solubility parameter. The solubility parameter of poly(vinyl alcohol) was varied from 12.6 to 10.6 by regulating the degree of hydrolysis. Polymer blends composed of HPL and poly(vinyl alcohol) (96% (δ=12.6), 88% (δ=11.8) and 75% (δ=10.6) hydrolyzed) formed homogeneous materials with no sign of phase separation or domains larger than 1500-2000 Å. It was concluded that hydroxyl groups on both polymers allows HPL (δ=11.1) to form at least partial miscible systems over a wider than expected range of solubility parameters.

The glass transition temperatures of HPL/PVA blends showed increasing T_g values with increasing HPL content. Uncharacteristically these blend T_g's were found to be higher than those of the parent polymers. This unusual trend was explained by the presence of strong hydrogen bonding between the hydroxyl groups of HPL and PVA. These strong hydrogen bonds act as quasi-crosslinks resulting in higher T_g values.

Introduction

Advances made in polymeric materials over the past decade have allowed them to replace conventional materials such as metals and metal alloys. This shift in choice of materials is based on economic advantages, simplified fabrication, freedom from corrosion, and lower weight. The trend toward use of polymeric materials will grow as the material science of this new technology is developed. One of the newest areas of interest in polymer science is that of polymer blends. The process of blending two polymers has been demonstrated to achieve specific properties at low cost (1-6). These specific properties are governed by the interaction of the two polymers. Two polymers may be considered "miscible" if they form a single, homogeneous phase and intimate mixing is achieved on a molecular level. On the other hand "compatibility" indicates the usefulness of a blend. Thus, immiscible blends do in certain cases exhibit good mechanical properties and are said to be mechanically compatible (7). Mechanical compatibility in immiscible blends is generally related to good interfacial adhesion between the phases of the blend constituents. In immiscible blends, specific interactions that occur between components will increase the overall entanglement of the polymers thus miscible blends have the assurance of mechanical compatibility.

The basic equation describing the state of miscibility of a two component system is given by

$$\Delta G_{mix} = \Delta H_{mix} - T\Delta S_{mix} \qquad \text{(Eq. 1)}$$

where ΔG_{mix} = Gibb's free energy of mix

ΔH_{mix} = Enthalpy of mixing

ΔS_{mix} = Entropy of mixing

T = absolute temperature

In order for a mixture to be miscible ΔG_{mix} must be negative. Thus, the miscibility of a two component mixture depends on the sign and magnitude of ΔH_{mix} and ΔS_{mix}. When dealing with polymer blends three of the most important parameters affecting the magnitude and sign of ΔH_{mix} and ΔS_{mix} are: 1) solubility parameter, 2) specific interactions, and 3) molecular weight. This study will focus on solubility parameter and specific interactions of lignin derivatives with PVA.

The solubility parameter δ is a measure of the cohesion of the material or the strength of molecular attraction between like molecules. The relationship between the solubility parameter and the enthalpy of mixing is given by the Hildebrand equation (8):

$$\frac{\Delta H_{mix}}{V} = (\delta_1 - \delta_2)^2 \phi_1 \phi_2 \qquad \text{(Eq. 2)}$$

where V = total volume of the mixture

$\delta_{1,2}$ = solubility parameters of component 1 and 2

$\phi_{1,2}$ = volume fraction of component 1 and 2.

This equation makes clear the concept that for two polymers to be miscible their solubility parameters should be closely matched. Equation 2 indicates that the predicted ΔH_{mix} is always positive or at best zero when the solubility parameters of the components are equal.

Thus the Hildebrand equation suggests that phase separation rather than miscibility is favored. However, many polymers have been reported to be miscible (1, 4). The mechanisms responsible for polymer-polymer miscibility are attributed to specific interactions between the two blend components. Specific interactions such as hydrogen-bonding, $n\pi$ and $\pi-\pi$ complex formation, charge transfer and ionic interactions have all been found experimentally to be responsible for miscibility in polymer blends (9). Considering that ΔH_{mix} values are the net result of breaking solvent (1-1) and polymer (2-2), (3-3) bonds and the creation of polymer-polymer (2-3) bonds, the importance of the solubility parameter and specific interactions between two polymers is clearly seen (10-11).

The overall goal of this study is to continue the on-going work at Virginia Tech to engineer plastics from lignin by employing the concepts of polymer blends. Emphasis will be placed on the effects of solubility parameter and specific interactions between polymers. The primary objectives of this study are as follows:

1) To blend hydroxypropyl lignin with three poly(vinyl alcohols) which have been hydrolyzed to the extent of 96%, 88% and 75%. By using the three different poly(vinyl alcohols) the number of hydroxyl groups PVA has available for hydrogen bonding can be regulated and PVA's solubility parameter is varied from 12.6 to 10.6.

2) To examine the morphology and thermal mechanical properties of these blends, and to describe their state of miscibility in terms of solubility parameter and the extent of interaction between the two

polymers.

Materials and Methods

I. Materials:

1) Hydroxypropyl lignin

A commercially available kraft lignin (Indulin AT from Westvaco Corporation, Charleston, South Carolina) was reacted with propylene oxide under alkaline conditions in toluene. This procedure has previously been described (12). The product of this reaction was isolated by liquid-liquid extraction with hexane and acetonitrile. The hydroxypropylated lignin derivative had a hydroxyl content of 6.5% and a glass transition temperature of 63.5°C (by DSC with heating rate of 10°C/min).

2) Poly(vinyl Alcohol)

Three commercially available poly(vinyl alcohols) with extents of hydrolysis of 96%, 88% and 75% were used in this study. Important parameters for each of these poly(vinyl alcohols) is listed below.

Poly(vinyl Alcohol)	T_g	δ	M_w
96% hydrolyzed	77°C	12.6	96,000
88% hydrolyzed	70°C	11.8	96,000
75% hydrolyzed	60°C	10.6	3,500
0% hydrolyzed	32°C	9.6	High

II. Methods

1) Solvent Casting of Blends

Separate 10% (w/w) solutions of each component were prepared using dimethylformamide (DMF). In order for the poly(vinyl alcohols) to

fully dissolve they had to be heated to 80°C. Once fully dissolved the solutions containing the two components were mixed together and allowed to stir at 80°C for two hours. This solution was poured into Teflon molds and the solvent was allowed to evaporate at room temperature for two days. The resulting films were then dried in a vacuum oven at 100°C for a week, and stored in a desiccator containing P_2O_5.

2) Scanning Electron Microscopy (SEM)

Fractured surfaces were observed using a AMR 900 scanning electron microscope. The samples were coated with 100 Å of Gold-Palladium to prevent charging. Samples were then observed at magnifications ranging from 500x to 5000x.

3) Differential Scanning Calorimetry (DSC)

DSC scans were run with a Perkin-Elmer DSC-4 instrument on samples weighing roughly 20 mg. Scans were started at a temperature of 30°C and heated at a rate of 10°C to a final temperature of 210°C, quenched and rescanned under the same conditions. All scans were run under a dry nitrogen atmosphere. The glass transition temperature (T_g) was defined as one-half the total change in heat capacity (Cp) occurring over the transition region. This method was used for both starting materials and polyblends.

4) Dynamic Thermal Mechanical Analysis (DMTA)

Dynamic thermal mechanical properties of the polyblends were determined using a Polymer Laboratories DMTA. Samples were tested as single cantalever beams with a free length of 1mm. The sample

dimensions varied in order that the log K value remained between 3.5 and 4. All samples were run at a heating rate of 5°C per min. and a frequency of 1 Hz.

Results and Discussion

1) SEM

A commonly used but qualitative technique for a quick determination of blend miscibility is through visual observation of the films. Generally a film of a miscible or compatible blend is clear, transparent and self-supporting. On the other hand, films of immiscible blends are usually diffuse and opaque. Although optical transparency might indicate miscibility, this criterion does not in all cases assure miscibility because the blend constituents may have matching refractive indices (13). All blends made with HPL and all three poly(vinyl alcohols) had lignin's characteristic brown color, but were transparent and self supporting. This indicates miscibility as discussed earlier.

Figure 1A shows a SEM micrograph of a poly(vinyl acetate) (0% hydrolyzed) blend containing 25% HPL. This blend shows distinct phase separation and distinct domains. On the other hand, Figures 1B, C and D show that poly(vinyl acetate) (96%, 88% and 75% hydrolyzed) blends containing 25% HPL have smooth fracture surfaces composed of a homogeneous material. No sign of phase separation or domains larger than 1500Å−2000Å, can be detected. Therefore under the given conditions, SEM results for poly(vinyl alcohol) blends containing HPL indicate that at least a partially miscible system exists, and that

miscibility is indicated. It is interesting to note that the range of solubility parameters for the poly(vinyl alcohols) used in this study was from 12.6 to 10.6 $(cal/cm^3)^{1/2}$, yet all blends containing these alcohols showed the same homogeneous morphology. Normally, miscibility is limited to $\Delta\delta$ values of $\pm$ 0.5 $(cal/cm^3)^{1/2}$. In compliance with this so called theory of matching solubility parameters poly(vinyl acetate), which has a solubility parameter of 9.6 exhibits distinct phase separation. Considering that hydroxypropyl lignin has a solubility parameter of 11.1 $(cal/cm^3)^{1/2}$ (varies depending on method of determination), the method of matching solubility parameters would suggest that HPL would be just as miscible in 96% hydrolyzed PVA (δ = 12.6) as in poly(vinyl acetate) (δ = 9.6) since they both have solubility parameters that are 1.5 $(cm^1/cm^3)^{1/2}$ from that of HPL. However SEM results indicate phase separation with poly(vinyl acetate) and miscibility for 96% hydrolyzed poly(vinyl alcohol). The reason for this difference is believed to be due to secondary association based on hydrogen bonding that can occur between the hydroxy groups found on both HPL and poly(vinyl alcohol), but that are not present in poly(vinyl acetate).

Thermal Properties

A) Differential Scanning Calorimetry (DSC)

Figure 2 shows a typical DSC scan of a HPL/poly(vinyl alcohol) blend. Blends containing 5%, 25% and 40% HPL all showed single T_g's and T_m's (for polyvinyl alcohol). However differences in the shape of the melting endotherms of 96%, 88% and 75% hydrolyzed PVA were

noticed. The 96% hydrolyzed PVA produced a sharp melt endotherm whereas the 88% hydrolyzed PVA produced a more rounded broad endotherm and 75% hydrolyzed PVA produced an even broader endotherm. This difference is attributed to the different degrees of crystallinity found in the polymers (14). The 96% hydrolyzed PVA has a more uniform chemical structure; thus it forms crystals that melt over a narrow range whereas 88% and 75% hydrolyzed PVA's have less uniform structures and their resulting crystalline structure melts over a broader range.

The area under the melt endotherm, in calories per gram of PVA, is plotted against HPL content in Figure 3. The area under the melt endotherm is a measure of the amount of energy that is needed to disrupt the crystalline structure of a polymer. In blends containing 96% hydrolyzed PVA and HPL a decrease in peak area is observed at 5% HPL content. At 25% HPL the peak area returns to that of pure 96% hydrolyzed PVA and remains at that point at 40% HPL content. On the other hand blends containing 88% and 75% hydrolyzed PVA show no change at a 5% HPL content; however a decrease in peak area is seen at a 25% HPL content. As with the 96% hydrolyzed PVA, blends containing 88% and 75% hydrolyzed PVA and 40% HPL showed peak areas equal to that of their respective pure PVAs. A reduction in the peak area indicates a change in the organization or extent of crystallinity in that material. In the case of polymer blends changes in crystalline structure can result from polymer-polymer interactions in the amorphous phase. Such interactions in the amorphous component cause

some disorder in the crystalline structure thus a reduction in the melt endotherm area is observed (15, 16). Therefore the observed reductions in melt endotherm area indicate the possibility of polymer-polymer interactions with HPL/PVA blends.

Analysis of the glass transitions for the HPL/PVA blends was made difficult due to the fact that the HPL had a T_g of 63.5°C and the 96%, 88% and 75% hydrolyzed poly(vinyl alcohol) had T_g's of 77°C, 70°C and 60°C, respectively. Typically clear analysis of polymer blends requires that the T_g's of the two polymers differ by at least 20 degrees so that, in the case of immiscibility, transitional smearing or overlapping will not hamper the observation of two T_g's (17). However in the case of HPL/PVA blends the maximum difference in T_g's is only 13.5 degrees C. Therefore it was not expected that any of the blends would show two T_g's. But analysis of the actual transition temperatures rather than the shape of the transitions will still provide information concerning the state of the HPL/PVA blends.

Theoretically miscible polymer blends will show T_g's that are intermediate to those of the parent polymers and follow models such as Flory-Fox or Gordon-Taylor (18,19). However in the case of HPL/PVA blends the T_g data did not follow any known models and T_g's above those of the parent polymers were observed. In order to describe this phenomenon the quotient of the experimental blend T_g divided by the predicted (Flory-Fox) T_g was graphed against HPL content, Figure 4. From Figure 4 we see that 96% and 88% hydrolyzed PVA show almost identical trends with virtually all of their data points having values

above one, which indicates that the experimental T_g's are higher than those predicted by the Flory-Fox equation. It is also apparent that the greatest deviation from the predicted T_g is seen at 25% HPL content. Deviations from linear models such as Flory-Fox have been reported in blends that are miscible or partially miscible, and these have been described as the result of strong specific interactions (20,21,22). Therefore it is believed that interactions are occurring between HPL and PVA, and the greatest interactions are observed at 25% HPL for 96% and 88% hydrolyzed PVA and at 40% HPL content for 75% hydrolyzed PVA. For the 88% hydrolyzed PVA blends this result correlates well with that seen with the melt endotherm data, which indicated a reduction in the energy needed to disrupt the crystalline structure of PVA at the 25% HPL level. However it should be pointed out that the 75% hydrolyzed PVA blends followed the 88% hydrolyzed PVA blends in terms of the melt endotherm data yet it did not follow the trend of 96% and 88% hydrolyzed PVA seen in Figure 4. The reason for this discrepancy is believed to be the result of molecular weight differences. The 96% and 88% hydrolyzed PVA have a molecular weight (M_w) of 96,000 whereas the 75% hydrolyzed PVA has a molecular weight (M_w) of 3,500. On the other hand, at a HPL content of 40%, the 75% hydrolyzed PVA blends show T_g's above the predicted T_g which once again is believed to be due to strong specific interactions.

These strong specific interactions are also believed to cause the blend T_g's to be higher than those of the parent polymers. The presence of strong interactions could result in an amorphous component

that coexists in a more closely associated state which could result in a reduction of free volume. Thus an increase in T_g is observed. Another explanation for this increase in T_g is suggested in studies performed on PVA gels. These gels are not gels in the classical sense since their crosslinks are formed not by primary chemical bonds (covalent bonds) but rather by secondary bonds such as hydrogen bonds (23). If such quasi crosslinks were formed in HPL/PVA blends in a large enough degree they could limit Brownian motion in the long chain molecules thus increasing the glass transition temperature.

B) Dynamic Mechanical Thermal Analysis (DMTA)

Figure 5 shows the tan δ curves for pure 96% hydrolyzed PVA and blends containing 5%, 25% and 40% HPL. Pure 96% hydrolyzed PVA shows a sharp α-transition at 88°C which is the result of large scale molecular motion in the amorphous phase. Also present is a shoulder centered at 130°C. This shoulder has been reported by several investigators and is the result of tortional or rotational motion of chains closely associated with the crystal lattice of poly(vinyl alcohol) (24,25,26). The PVA (96% hydrolyzed) blend containing 5% HPL shows that the α-transition has shifted from 88°C for pure PVA to 92°C for the blend. The peak width at one half peak height has become greater during blending. This increase in peak width causes the distinct shoulder that was seen with pure 96% hydrolyzed PVA to become non-distinct. Likewise blends consisting of 25% and 40% HPL also experience peak broadening and increases in tan δ-transition temperature to 96°C and 105°C, respectively. These non-typical

increases in tan δ-transition temperatures, which are synonymous to glass transition temperatures, can be explained by the same mechanisms used to explain the T_g data produced by DSC. That being, the presence of strong interactions cause the amorphous components to coexist in a more closely associated state and the ability of these interactions to act as quasi-crosslinks which would limit molecular mobility. This possibly explains the existence of a blend T_g above that of the parent polymers.

The presence of peak broadening with the addition of HPL indicates that varying degrees of miscibility possibly exist between HPL and 96% hydrolyzed PVA. A very narrow tan δ-transition would indicate that a polymer experiences a uniform environment and thus relaxes over a narrow temperature range. However in the case of partially miscible blends a polymer can experience environments associated with polymer (1-1) interphases and varying degrees of polymer (1-2) interphases. These different environments would cause polymer relaxations to occur over a broader range resulting in a broadening of the tan δ-transition (2).

Figure 6 shows the log storage modulus curves for pure 96% hydrolyzed PVA and blends consisting of 96% hydrolyzed PVA and 5%, 25% and 40% HPL. Pure 96% hydrolyzed PVA experiences a sharp transition from the glassy state to the rubbery state which is typical for homogeneous amorphous polymers. However blends consisting of 5% and 25% HPL show modulus transitions that occur very gradually over a larger temperature range, which is classically how partially miscible

blends perform (27). On the other hand at 40% HPL content the modulus transition occurs over a narrower range than that experienced by blends consisting of 5% and 25% HPL. This indicates that the blend consisting of 40% HPL may be more miscible than the blends containing 5% and 25% HPL.

Blends consisting of 75% hydrolyzed PVA and HPL showed the same trends that were seen with 96% hydrolyzed PVA. Those trends being, an increase in blend T_g with increasing HPL content and an increase in tan δ-transition width with increasing HPL content. However blends consisting of 88% hydrolyzed PVA did not follow the same trends as those found with 96% and 75% hydrolyzed PVA. As seen in Figure 7 the T_g of the blend did not consistently increase with increasing HPL content. Though the relatively small changes in T_g that occurred between pure PVA and blends containing 5% and 25% HPL may make this difference insignificant. The major difference between the blends containing 88% hydrolyzed PVA and those containing 96% and 75% hydrolyzed PVA is in their relationships between the tan δ-transition width and percent HPL, illustrated in Figure 8. In order to normalize the data to those of the respective starting materials the ordinate in Figure 8 indicates the quotient of the blend tan δ-transition width divided by the tan δ-transition width of the pure PVA used in that blend. Therefore a value of one on the ordinate indicates that the tan δ-transition width of the blend is the same as that of the pure PVA used in that blend. A value less than one indicates a tan δ-transition width that is smaller than that of the pure PVA used in that blend.

The shaded areas on the graph indicate the range in which the data was found; the minimum and maximum limits of the range are dictated by actual data points.

From Figure 8 it is clear that blends consisting of 88% hydrolyzed PVA showed blend tan δ-transitions that were consistently more narrow than that of pure 88% PVA. By contrast blends containing 96% and 75% hydrolyzed PVA and HPL showed tan δ-transition that were consistently broader than those of their respective PVA's. The fact that blends containing 88% hydrolyzed PVA had consistently more narrow tan δ-transitions indicates that these blends had a greater degree of miscibility than that for blends containing 96% and 75% hydrolyzed PVA. The mechanism responsible for this increased miscibility is believed to be related to both solubility parameter and polymer interactions.

The solubility parameter for HPL is believed to be around 11.1 $(cal/cm^3)^{1/2}$, however it may be lower or higher depending on the method of determination. If it is assumed to be slightly higher the concept of matching solubility parameters would predict at least a partially miscible system for blends of 88% hydrolyzed PVA and HPL, since 88% hydrolyzed PVA has a δ of 11.8 $(cal/cm^3)^{1/2}$. With the combination of closely matched solubility parameters and the ability to form hydrogen bonds one would predict a high degree of miscibility for blends consisting of 88% hydrolyzed PVA and HPL. On the other hand since 96% and 75% hydrolyzed PVA's are the upper and lower limits in terms of solubility parameters for this experiment the concept of

matching solubility parameters would predict that blends containing these PVA's would have very limited miscibility. However the ability of these polymers to form hydrogen bonds with HPL is believed to cause at least partially miscible systems. The ability of 96% hydrolyzed PVA to form more hydrogen bonds than 75% hydrolyzed PVA enables it to show consistently narrower tan δ-transitions than 75% hydrolyzed PVA blends thus indicating greater miscibility.

Conclusions

1) Polymer blends composed of HPL and poly(vinyl alcohol) (96%, 88%, and 75% hydrolyzed) formed homogeneous materials with no sign of phase separation or domains larger than 1500-2000Å. Therefore HPL/PVA blends form at least partially miscible systems.

2) The PVA's used in this study had solubility parameters that ranged from 12.6 to 10.6 $(cal/cm^3)^{1/2}$, yet all blends containing these alcohols showed the same homogeneous morphology. Hydroxypropyl lignin has a solubility parameter of roughly 11.1. This exceeds the normal limit of $\Delta\delta$ ($\pm$0.5) that determines miscibility. Therefore it is believed that hydrogen groups on both polymers allows HPL to form at least partial miscible systems over a wider than expected range of solubility parameters.

3) The presence of interactions, hydrogen bonding, was suggested by a decrease in melt endotherm area observed with a number of the HPL/PVA blends. A reduction in melt endotherm area indicates a change in the organization or extent of crystallinity in that material. In HPL/PVA blends changes in the crystalline structure are believed to result from polymer-polymer interactions in the amorphous phase.

4) The glass transition temperatures of HPL/PVA blends showed increasing T_g values with increasing HPL content. Uncharacteristically these blend T_g's were found to be higher than those of the parent polymers. This unusual trend was explained by the presence of strong hydrogen bonding between the hydroxyl groups of HPL and PVA. These strong H-bonds act as quasi-crosslinks resulting in higher T_g values.

5) In the DMTA analysis of PVA/HPL blends changes in the shape of the tan δ-transitions indicated that blends containing 96% and 75% hydrolyzed PVA experienced increases in tan δ-transition breadth with increasing HPl content. Such increases in tan δ-transitions are believed to indicate that the blend is becoming more immiscible with the addition of HPL. However blends containing 88% hydrolyzed PVA showed more narrow or constant tan δ-transitional breadths with increasing HPL content. This behavior was described as the result of a greater degree of miscibility than that observed with 96% or 75% hydrolyzed PVA. The mechanism responsible for this increased miscibility is believed to be a combination of closely matched solubility parameters and polymer-polymer interactions.

LITERATURE CITED

1) O. Olabisi, L. M. Robeson, and M. T. Shaw, "Polymer-Polymer Miscibility", Academic Press, New York (1979).

2) D. Klempner and K. C. Frisch (eds.), "Polymer Alloys", Plenum Press, New York (1980).

3) S. L. Cooper and G. M. Estes (eds.), "Multiphase Polymers", Adv. Chem. Ser., 176 (1979).

4) D. R. Paul and S. Newman (eds.), "Polymer Blends", Vol. 1 land 2, Academic Press, New York (1978).

5) D. R. Paul and J. W. Barlow, J. Macromol. Sci., Rev. Macromol. Chem., C18, 1, 109 (1980).

6) J. A. Manson and L. H. Sperling, "Polymer Blends and Composites", Plenum Press, New York (1976).

7) "Polymer Blends," Polym. Eng. Sci. 22(2) (1982).

8) J. H. Hildebrand and R. L. Scott, "The Solubility of Non-Electrolytes," Dover, New York, 1964.

9) J. W. Barlow and D. R. paul, Polym. Eng. Sci., 21(15), 985 (1981).

10) G. Scatchard, Chem. Rev. 8, 321 (1931).

11) J. H. Hildebrand, J. M. Pravsnitz, and R. L. Scott, "Regular and Related Solutions", Van Nostrand Reinhold, New York, 1970.

12) L. C. F. Wu and W. G. Glasser, J. Appl. Polym. Sci., 29, 1111 (1984).

13) A. J. Yu, in "Copolymers, Polyblends and Composites," (N.A.J. Platzer, ed.), Adv. Chem. Ser., 142, 2 (1975).

14) R. Greco, in "Polymer Blends and Mixtures," D. J. Walsh, J. S. Higgins and A. Maconnachie, ed.), NATO ASI series, pp. 453 (1985).

15) W. Wenig, F. E. Karasz and W. J. MacKnight, J. Appl. Phys., 46, 4166 (1975).

16) R. Hammel, W. J. MacKnight, and F. E. Karasz, J. Appl. Phys., 46, 4199 (1975).

17) F. E. Karasz, in "Polymer Blends and Mixtures," (D. J. Walsh, J. S. Higgins and A. Maconnachie, ed.), NATO ASI series, pp. 25

(1985).

18) T. G. Fox, Bull. Am. Phys. Soc., 1, 123 (1956).

19) M. Gordon and J. S. Taylor, J. Appl. Chem., 2, 493 (1952).

20) D. R. Paul, Org. Coat. Prepr., 50, 187th National ACS Meeting, St. Louis, (April 1984).

21) T. K. Kwei, Appl. Polym. Sci. 22, 307-313 (1984).

22) E. P. Otoeka, and T. K. Kwei, Macromolecules 1, 244 (1968).

23) M. Watase, et al. Polymer Communications. Vol. 24, Sept. 1983, p. 270-272.

24) K. Shirakashi, K. Ishikawa, K. Miyasaka, Kobunshi Kagaku., 1964, 21, 588.

25) A. Nagai, and M. Takayanagi, Rept. Prog. Polym. Phys. Jpn. 1964, 8, 249.

26) Y. Wada, K. Tsuga, K. Arisawa, Y. Ohzawa, K. Shida, and T. J. Nishi, Polym. Sci., 1966, 15, 101.

27) R. G. C. Arridge, "Mechanics of Polymers", Clarendon Press, Oxford University, 1975.

List of Figures

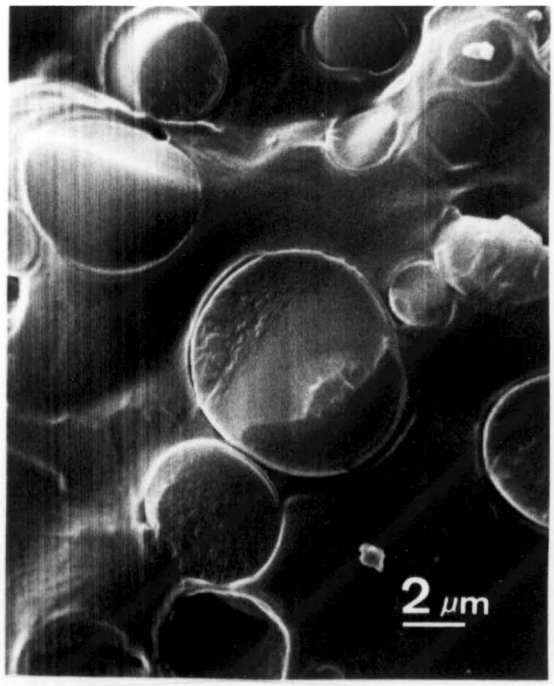

Figure 1 (A) 25% HPL / 75% Poly (Vinyl Acetate) 5000 X

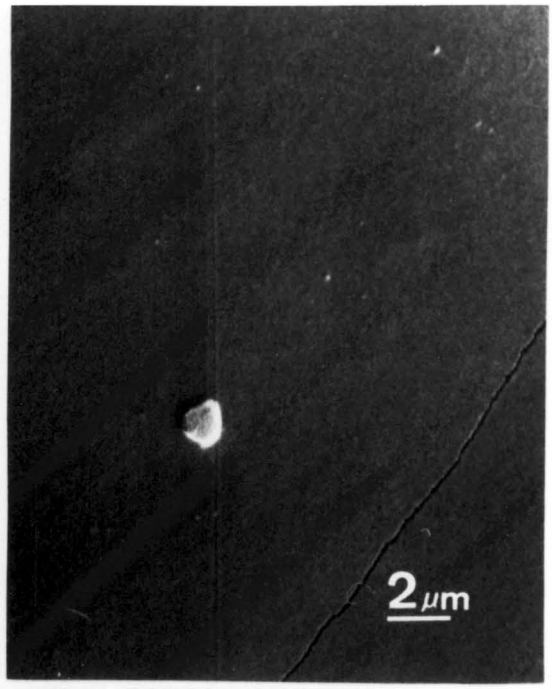

Figure 1 (B) 25% HPL / 75% Poly (Vinyl Acetate) 75% Hydrolyzed 5000 X

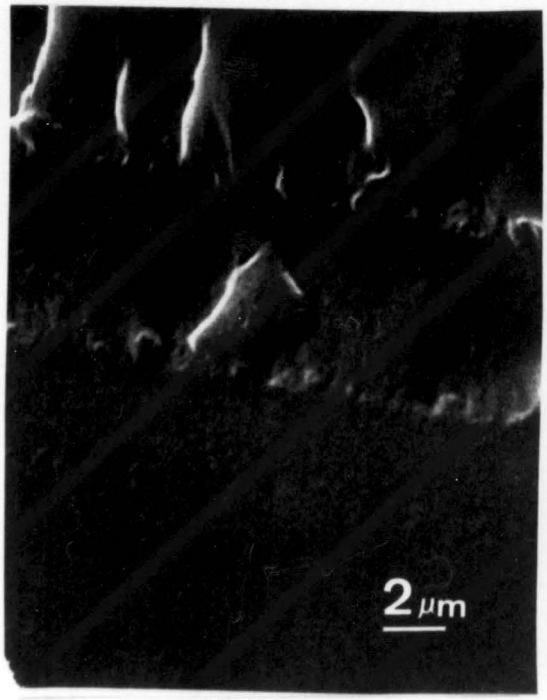

Figure 1 (C) 25% HPL / 75% Poly (Vinyl Acetate) 88% Hydrolyzed 5000 X

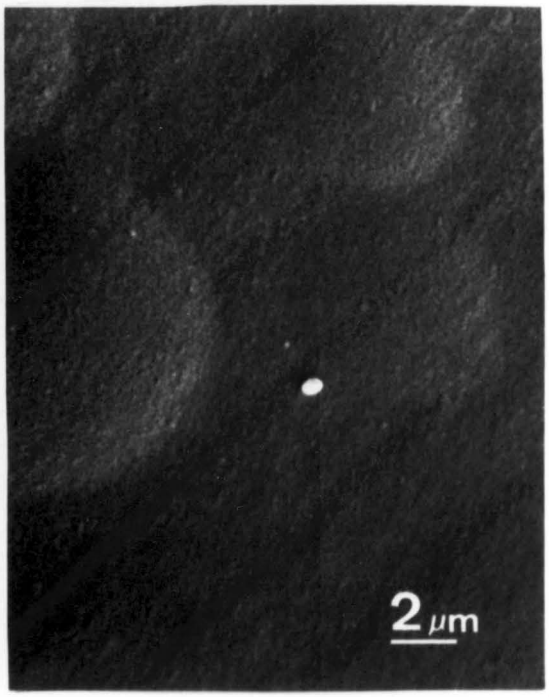

Figure 1 (D) 25% HPL / 75% Poly (Vinyl Acetate) 96% Hydrolyzed 5000 X

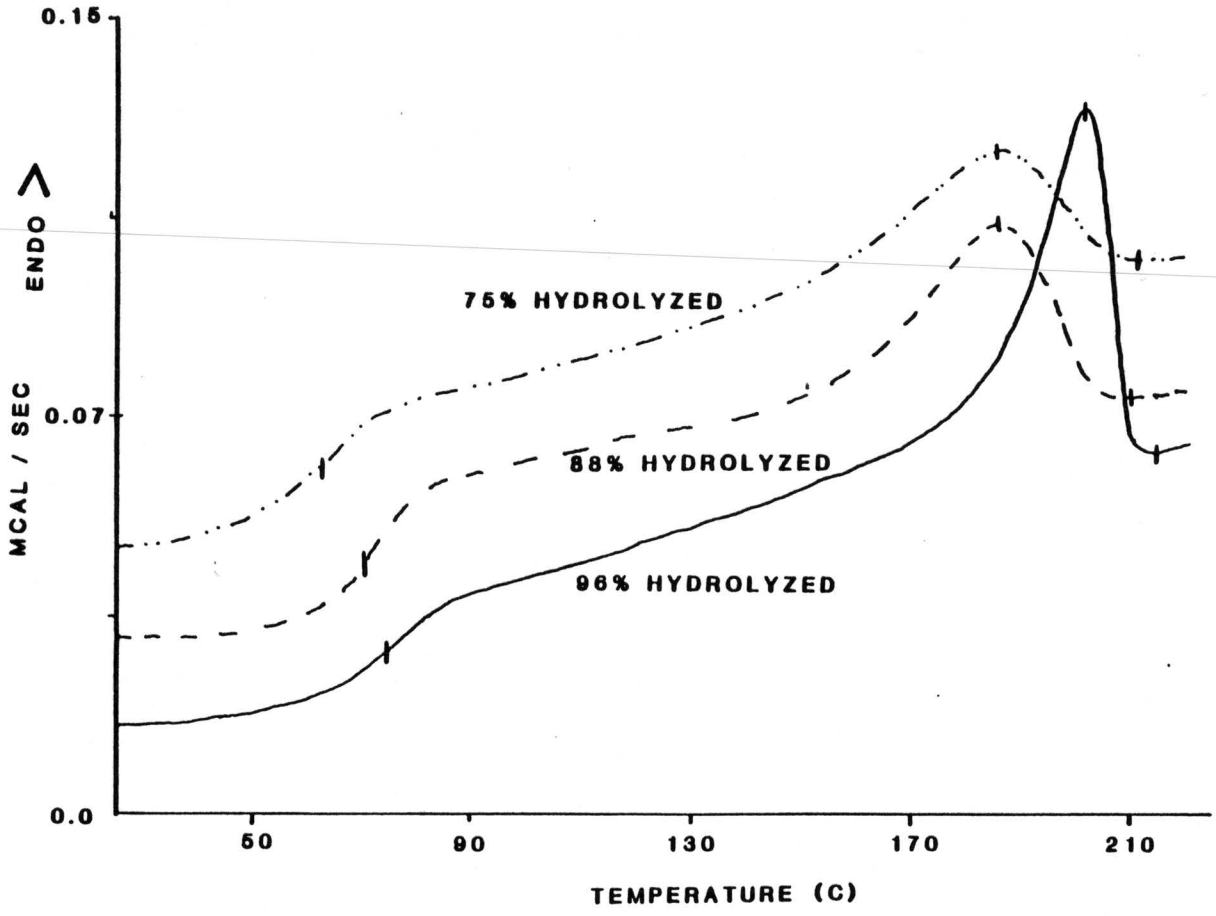

Figure 2. The DSC trace of blends containing 25% HPL, 75% PVA

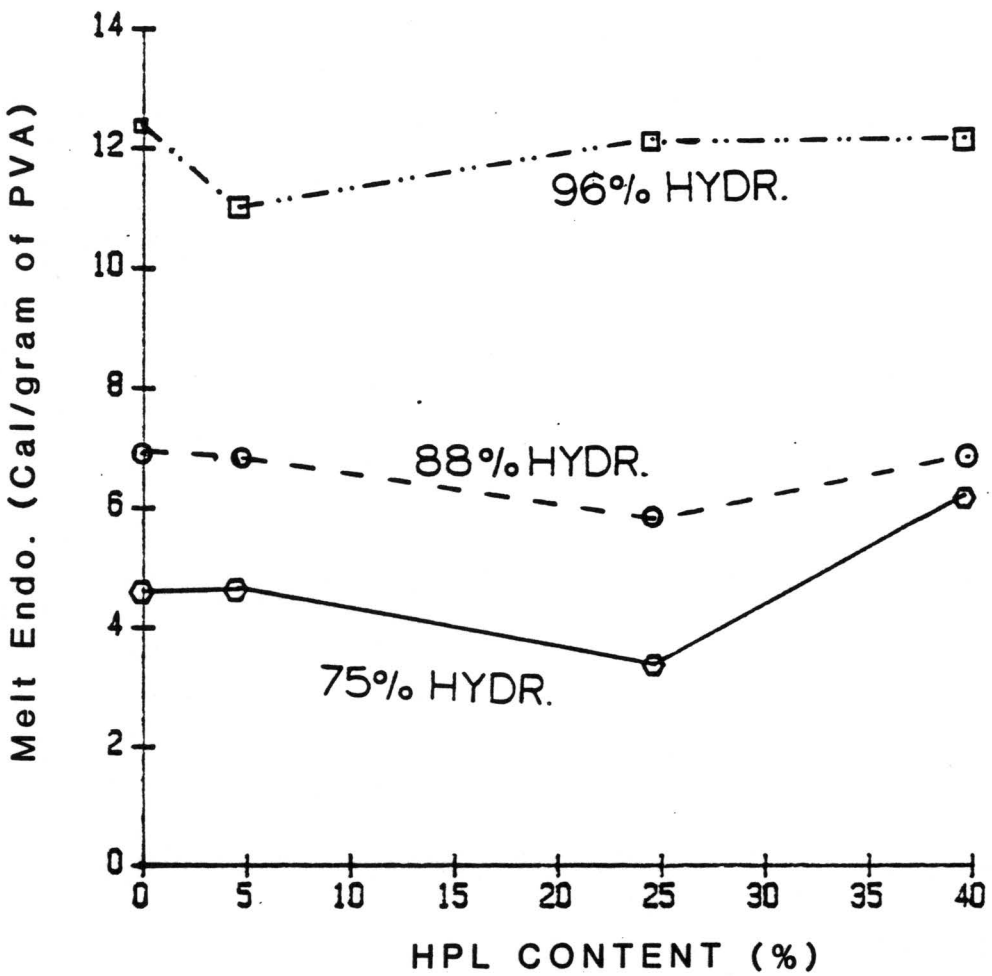

Figure 3. The variation of PVA's melt endotherm with the addition of HPL.

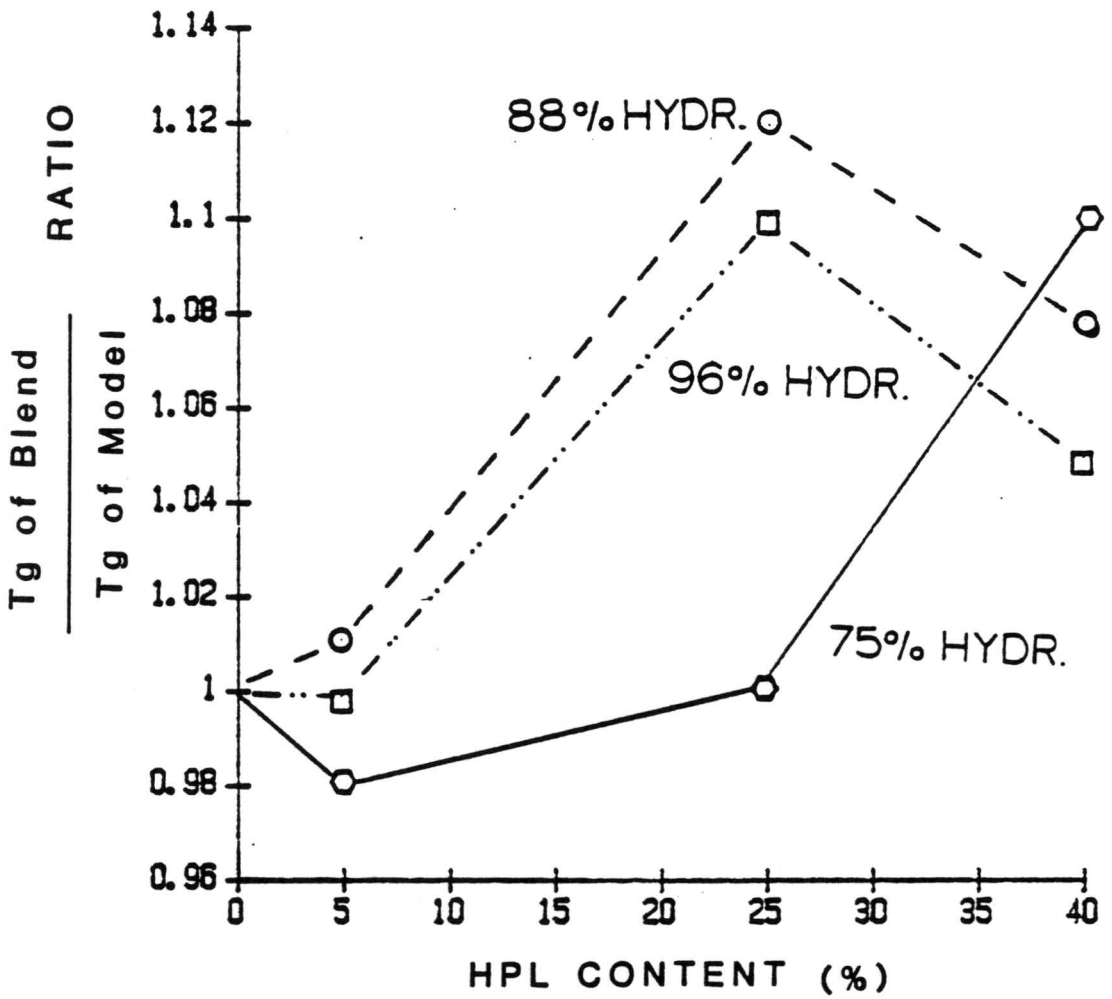

Figure 4. The variation of the ratio (T_g of blend)/(T_g of model) with the addition of HPL.

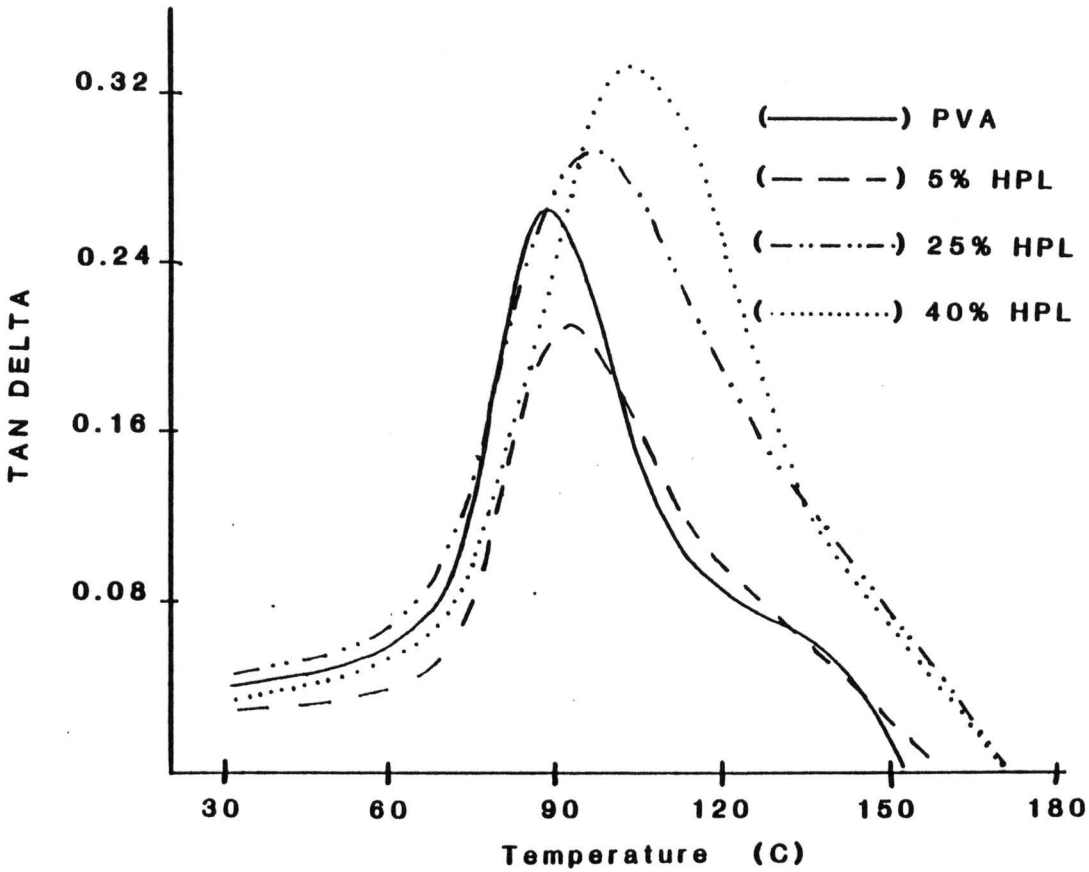

Figure 5. The variation in tan with temperature for HPL/PVA (96% hydrolyzed) blends where (——) pure PVA, (– –) 5% HPL, (·· –) 25% HPL, and (·····) 40% HPL.

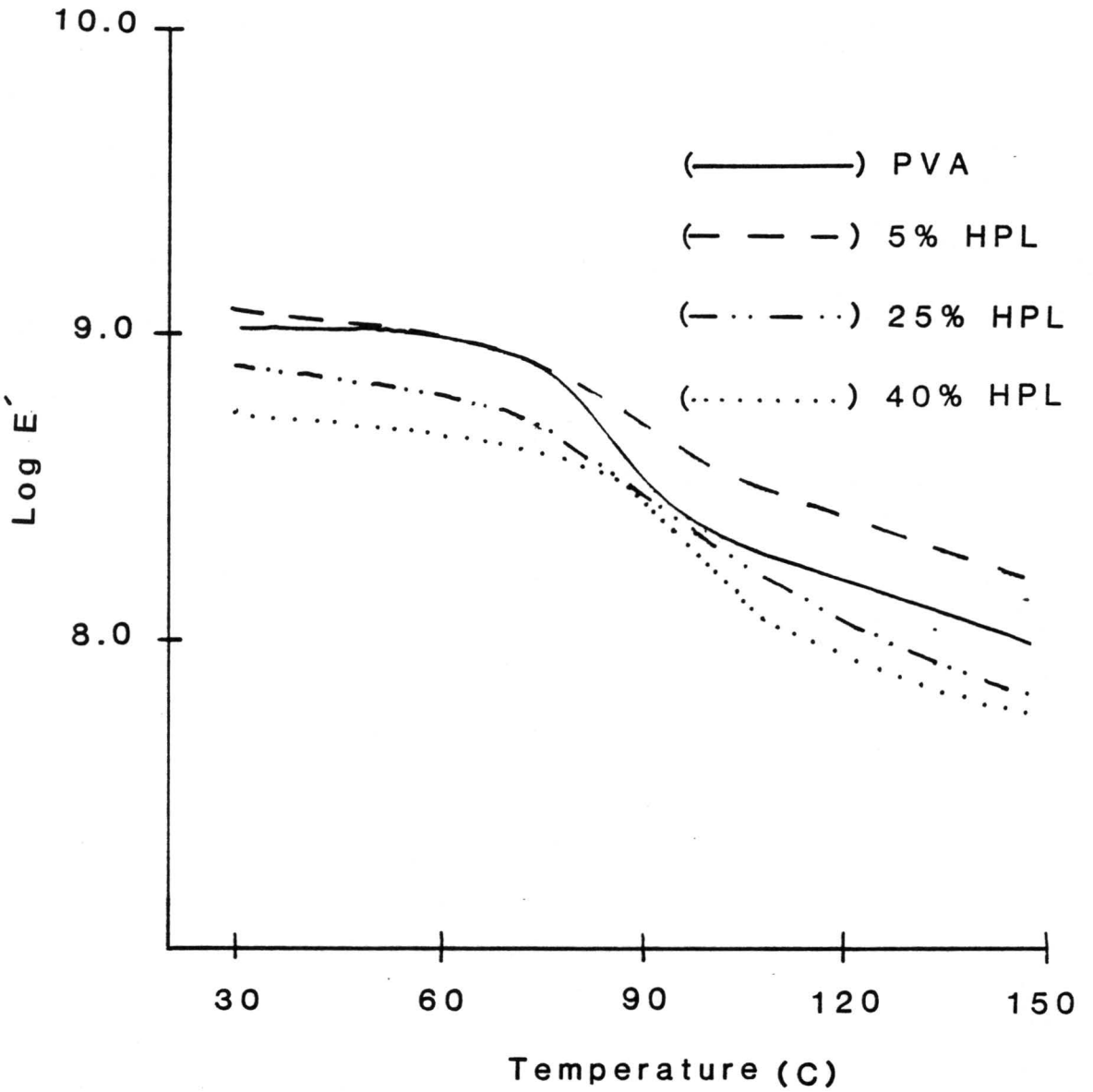

Figure 6. The variation in storage modulus (E') with temperature for HPL/PVA (96% hydrolyzed) blends where (——) pure PVA, (- -) 5% HPL, (- · ·) 25% HPL, and (· · · ·) 40 HPL.

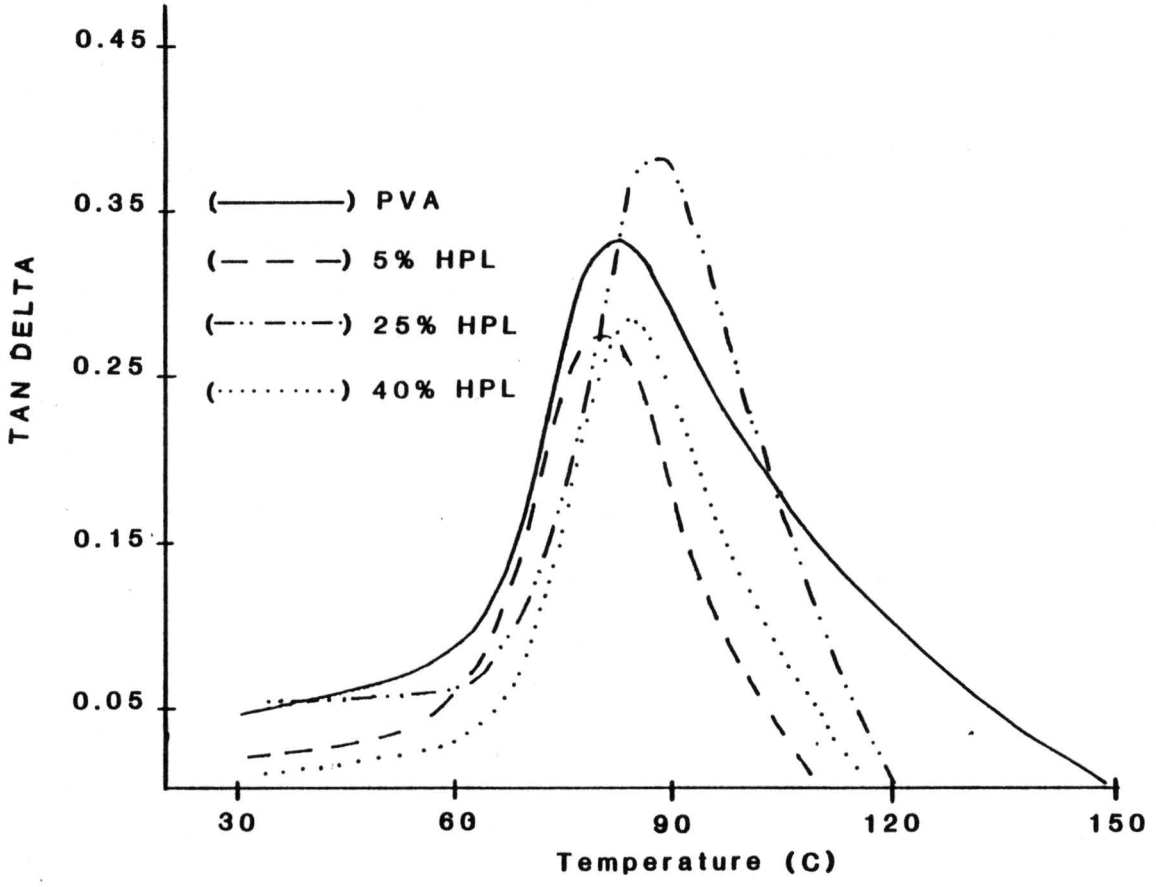

Figure 7. The variation in tan δ with temperature for blends containing HPL/PVA (88% hydrolyzed) where (——) pure PVA, (--) 5% HPL, (—··) 25% HPL and (····) 40% HPL.

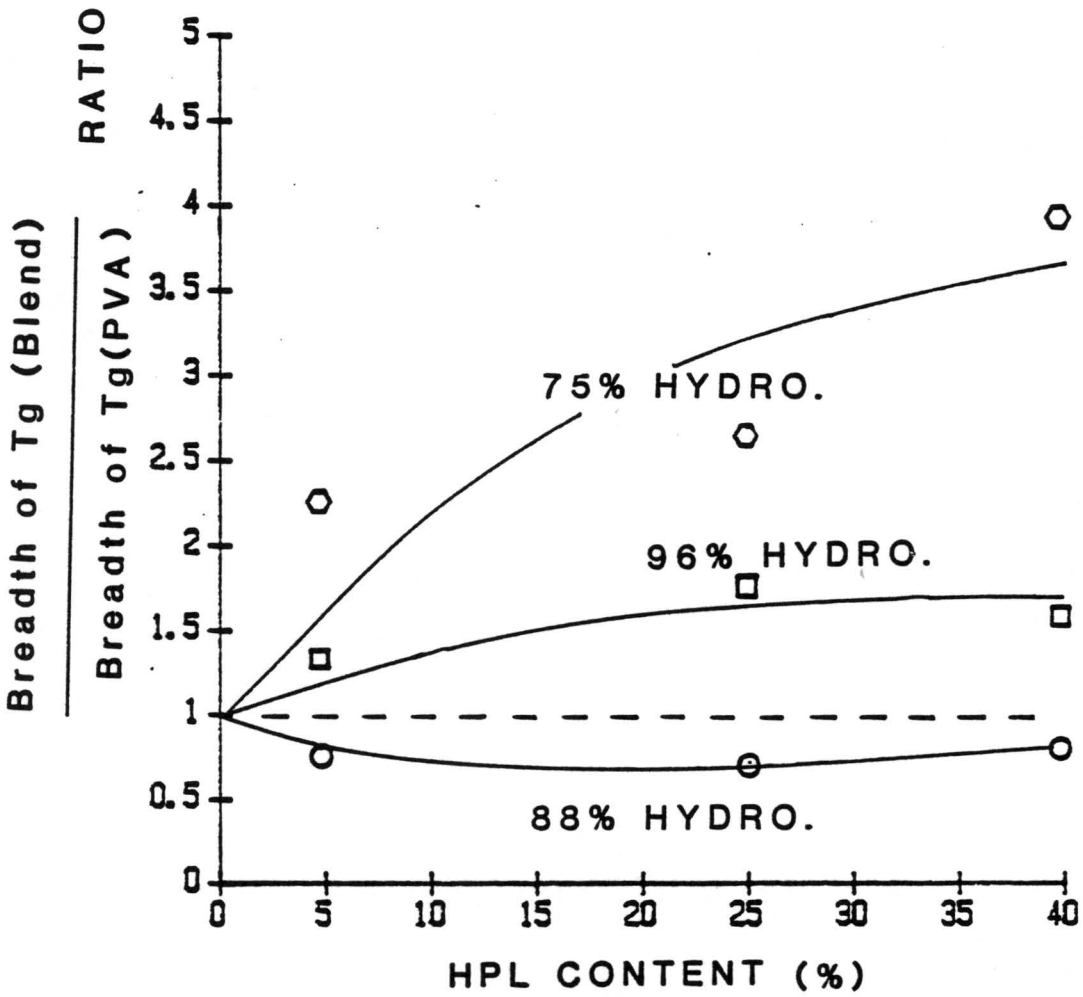

Figure 8. The variation of the ratio (blend T_g breadth)/(PVA T_g breadth) with the addition of HPL.

The vita has been removed from the scanned document